Evaluation of gasification efficiency of glucose and sorbitol under hydrothermal reforming conditions in an autoclave batch reactor

M.J.W. Blom

June 29, 2015

Abstract

Gasification of biomass is an interesting method for converting biomass to calorific gas. Studies on glucose, a model component for biomass have shown that when this is attempted at temperatures below the critical temperature of water, char formation takes place. Other studies suggest that stabilisation of biomass by hydrogenation could prevent char formation. This report focuses on sorbitol, a model component for hydrogenated biomass, in combination with glucose. Non-catalytic conversion in a 45 ml autoclave batch reactor is described. It was found that sorbitol is stable up to at least 250 °C for at least 30 minutes. It was also found that at 350 °C destruction of sorbitol takes place and possible mechanisms are discussed. Reaction products were found to be various aqueous and oil. Dissolved organics in the aqueous phase were identified by extraction and GC-MS. Gaseous components were identified by Micro-GC. Dependences of sorbitol destruction, oil formation and gas production on residence time were researched. It was found that all increase with temperature. Char formation for glucose experiments was found to be dependent on temperature and glucose/sorbitol fraction and residence time. Char formation increases with temperature and residence time, and shows disputable results for glucose/sorbitol fraction.

Contents

Chapter 1

Introduction

Most of the world demand of energy is supplied by fossil fuels. Resources are likely to be sufficient for the upcoming decades, but there is a widespread doubt about the desirability to remain dependent on fossil fuels [1]. The combustion of coal, oil and natural gas causes the emission of greenhouse gases which leads to global warming [2]. Moreover, fossil fuels are largely located in politically unstable areas and will eventually run out. This has led many national governments and multinationals to pursuit alternative and renewable energy sources [3]. Biomass is the most common form of renewable energy and is currently being rediscovered as an energy source [4]. A challenge in the conversion of biomass to energy is that biomass usually contains a lot of water, which requires a substantial amount of energy to vaporise. A promising method to turn biomass into calorific gas is by aqueous-phase reforming (APR) [3].

The model component for biomass is glucose, since it's the monomer of the polysaccharide cellulose. It has been found that upon gasification of glucose, significant coke formation is present at glucose concentrations above 10% [5], which poses a problem as it leads to plugging of the reactor and reduces yield. When glucose is hydrogenated, it forms sorbitol, a polyalcohol. The aqueous phase reformation of sorbitol results in higher gas yields [6] and lower char formation tendency in comparison with glucose [3]. It has already been shown that when a hydrogenation reactor is placed before a catalytic APR reactor, glucose can be converted to sorbitol and then reformed [6]. Its however not yet known what happens when a combination of glucose and sorbitol solution is fed to a reforming reactor. This data is however relevant, because it determines to what extend glucose needs to be hydrogenated for high concentration gasification.

This bachelor thesis is part of a larger research, which is still in it's early phase. The larger research is based on the findings that a mild hydro-treating results in the stabilisation of biomass, reducing char production. The ultimate goal of that research is to build a set-up of two stages, with the hydrogenation of biomass in the first and gasification of that biomass in the second. Reactions should there occur at sub-critical temperatures, to improve energy efficiency. In order to accomplish this, first reaction characteristics of model biomass and stabilised biomass components, glucose and sorbitol, need to be determined and proof of principle for sorbitol must be given. To do this, this research tries to determine the stability of sorbitol for different temperature, reaction products of sorbitol does react and tries to identify reactions that occur. Another goal for this research is to identify a concentration of glucose in sorbitol solution that doesn't produce char and to find the influence of sorbitol presence on char formation.

Chapter 2

Literature review

In the 1970's the decomposition of organic compounds in hot compressed water was studied at the Massachusetts Institute of Technology (MIT). It was observed that the reaction produced a lot of tar under sub-critical conditions. However, when the reaction was performed with pressure and temperature above their critical values, the tar disappeared completely, which kick-started the research and developments on supercritical water oxidation (SCWO) [7]. For water to reach it's critical state, the temperature needs to be above 374 °C and the pressure above 22.1 MPa [8], as shown in figure 2.1. Those reaction conditions however demand a lot of energy for heating and high material cost to cope with the pressure for a potential plant. Therefore it's desirable to find a reaction window for sub-critical conditions in which tar formation doesn't take place, but catalytic conversion can.

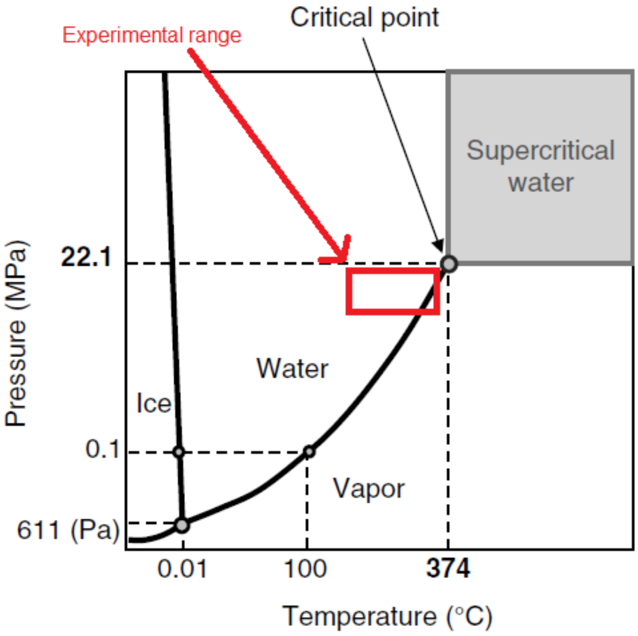

Figure 2.1: Phase diagram of water showing critical region and experimental range

2.1 The effect of temperature on APR

Hydrothermal gasification can be subdivided into three main categories, based on temperature. A high temperature region of above 500°C, a medium temperature region between the critical temperature (T_c) and 500°C and a sub-critical region below T_c [7]. In the high temperature range, the main gaseous product is hydrogen, versus methane for medium temperatures and various gasses and small molecules for sub-critical temperatures. Furthermore a change in intermediate products found after reaction is apparent between 600-650 °C [9]. Both the shift in gaseous products and intermediate products will be outlined below.

2.1.1 Temperature influence on product gasses

The products of the complete hydrothermal reformation, without other reactions of an organic substance are determined by it's molecular formula. For glucose that is $C_6H_{12}O_6 + 6H_2O \rightarrow 6CO_2 + 12H_2$ [10] and for sorbitol that would be $C_6H_{14}O_6 + 6H_2O \rightarrow 13H_2 + 6CO_2$ [11]. This idealised stoichiometric reaction implies that only hydrogen and carbon dioxide would be produced. It is however known that organic acids are intermediates in glucose gasification and that alcohols and some acids are a intermediates in sorbitol gasification as explained in section 2.2. Those organic acids and alcohols can decompose further via CO as an intermediate or be reformed to alkanes. [12, 13].

The CO formed can react in an number of ways, but the most important ones for product gas composition are the water-gas-shift (WGS) reaction 2.1 and the methanation reaction 2.2 [9, 14]. With an increasing temperature, it is observed that the equilibrium composition of product gasses switches towards more hydrogen production, due to the WGS reaction [15, 9, 16]. The exact temperature at which hydrogen production becomes the dominant factor is dependent on the catalytic activity of the reactor wall [17], on which will be elaborated in section 2.6. It is also observed that the carbon efficiency (CE) defined as the degree of conversion of carbon from biomass increases with temperature and can reach the theoretical maximum of 100 % for dilute solutions (less than 2 wt.% organics) [15, 9, 16, 18, 19].

$$CO + H_2O \rightarrow H_2 + CO_2 \tag{2.1}$$

$$CO + 3H_2 \rightarrow CH_4 + H_2O \tag{2.2}$$

2.1.2 Temperature influence on liquid products

Glucose

The product composition after glucose gasification can be divided into two regimes for non-catalytic gasification: A regime at temperatures above 650 °C and below 650 °C. In the upper regime, mostly acetic acid and some butanoic acid are found in relatively low concentration in the liquid phase [9]. In the lower temperature regime, lots of different products are found in the liquid phase [9, 20, 21, 22]. A GC/MS spectrum containing the main liquid products at 600 °C is shown in figure 2.2.

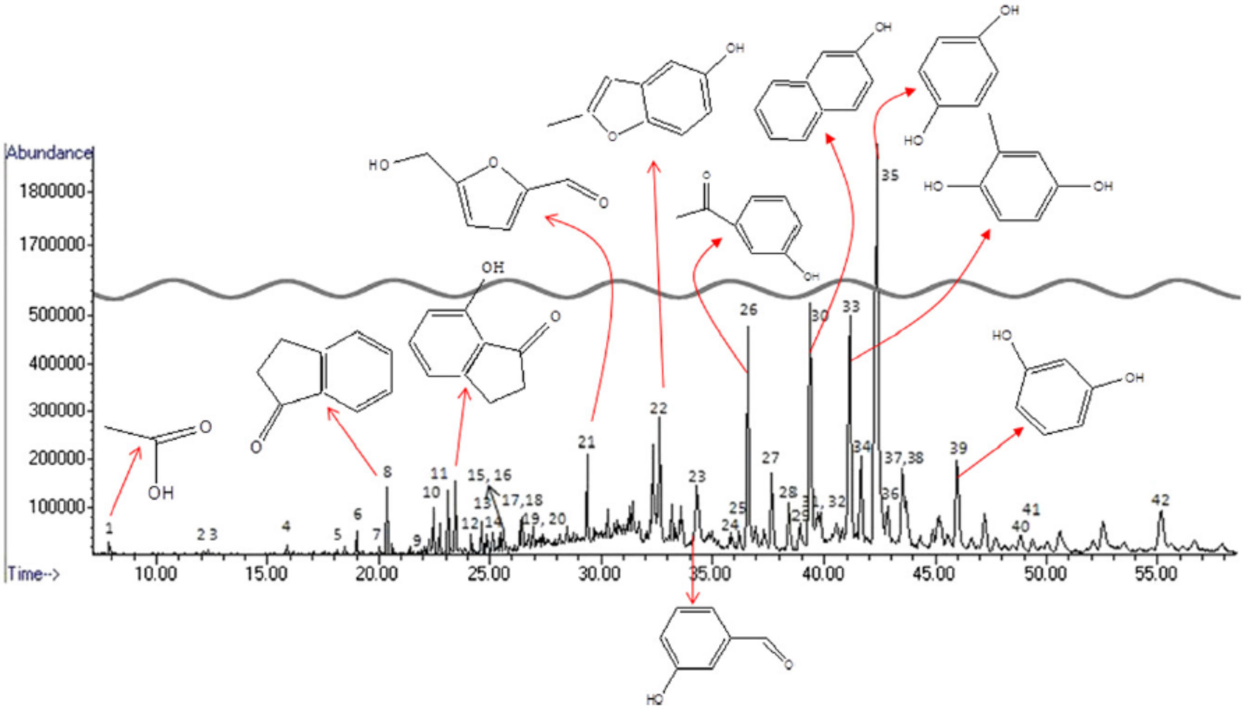

Figure 2.2: Compounds in liquid phase after reforming at 600°C and 25 MPa, 3.6 wt% glucose. Adapted from Susanti et al.[9]

Sorbitol

The behaviour of sorbitol in aqueous phase reforming differs from that of glucose. When sorbitol is reformed, more of its carbon atoms end up in the gas phase [18]. The reaction pathways differ as well, thus resulting in a different liquid product composition. With aqueous phase reforming under sub-critical conditions over a catalyst, a large variety of products is obtained[19, 13], as seen in figure 2.3. The exact product composition depend on the catalyst used[17]. An example of liquid products that are found after low temperature catalytic gasification of sorbitol, can be seen in figure 2.6. Literature doesn't mention experimentally found reaction products for non-catalytic hydrothermal gasification of sorbitol, however figure 2.6, based on other literature.

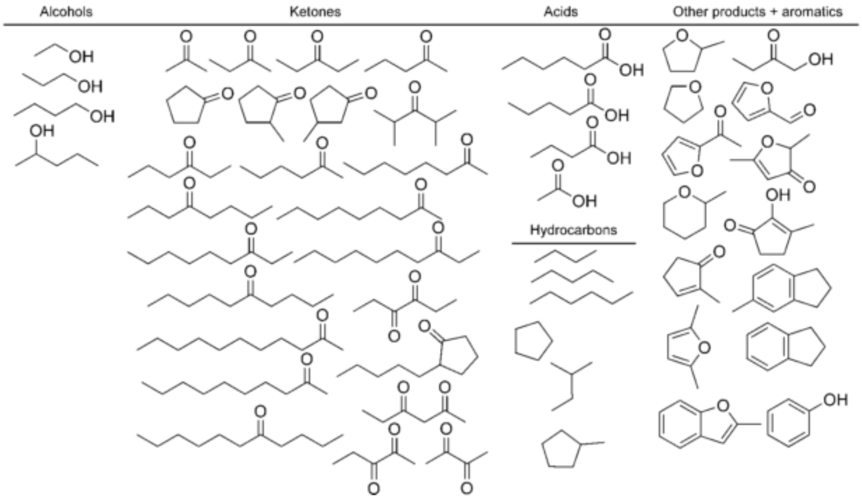

Figure 2.3: Compounds in liquid phase after reforming under sub-critical conditions. Adapted from Kirilin et al.[19]

2.2 Reaction pathways

2.2.1 Glucose

There is a lot of agreement in literature about the reaction pathways that lead to the formation of gaseous and liquid products in SCWG of glucose. The main reactions are outlined in figure 2.4 and will be explained in detail below. A literature study has been performed by Aida et al. to compile a detailed set of reactions that occur in SCW, as seen in figure 2.5 [22]. It has been observed that the transformation of glucose to fructose readily takes place at subcritical and supercritical conditions, but the reverse reaction is negligible [24]. The acids that are formed in the reactions are further gasified via an O-H scissioning and consecutive β scissioning or react to form tar [12]. As described in section 2.1 only at higher temperatures, the liquid products will fully react, which implies that the intermediate products shown in figure 2.5 are quite stable.

As can be seen in figure 2.5, glucose can react via a number of pathways. From it's closed ring structure it can react directly to furfural and formaldehyde. The open chain form of glucose can undergo a retro aldol reaction to form erythose and glycolaldehyde. A rearrangement of open chain glucose leads to form 2a, which can also undergo retro aldol and various other reactions. Fructose, which is formed within two seconds of the reaction [24], dehydrates to 5-(hydroxymethyl)furfural (5-HMF), which may react further to form various acids and ketones, and aromatic 1,2,4-Benzenetriol.

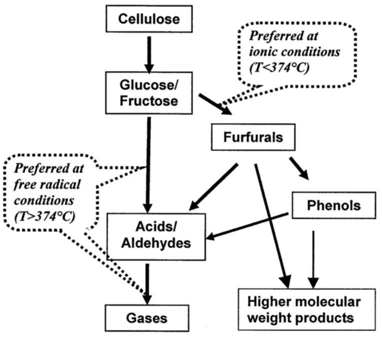

Figure 2.4: Simplified reaction scheme for the gasification of glucose. Adapted from Kruse et al. [23]

2.2.2 Sorbitol

Sorbitol is the hydrogenated version of glucose. It lacks the aldehyde group, seen in the open chain form of glucose and it has another alcohol group at that place. Literature mentions a lot of data on aqueous phase reforming of sorbitol over Pt/Al_2O_3 catalyst in sub-critical conditions [19, 13, 11, 25]. The reaction scheme shown in figure 2.6 shows a diagram which is solely based on literature, but should show non-catalytic reactions. Other products are however formed, as shown in figure 2.3, depending on the catalyst used. A proposed catalytic reaction path is seen in figure 2.7. For non-catalytic reforming of sorbitol, little experimental information is known about product composition. It is however known that nickel, a component in the reactor wall also exhibits catalytic activity in sorbitol reforming [17].

2.3 Coke formation

In the gasification of biomass or model compounds for biomass, the formation of coke and tar poses a significant problem, as it leads to lower gasification efficiency and reactor plugging. Two kinds of coke can be distinguished:

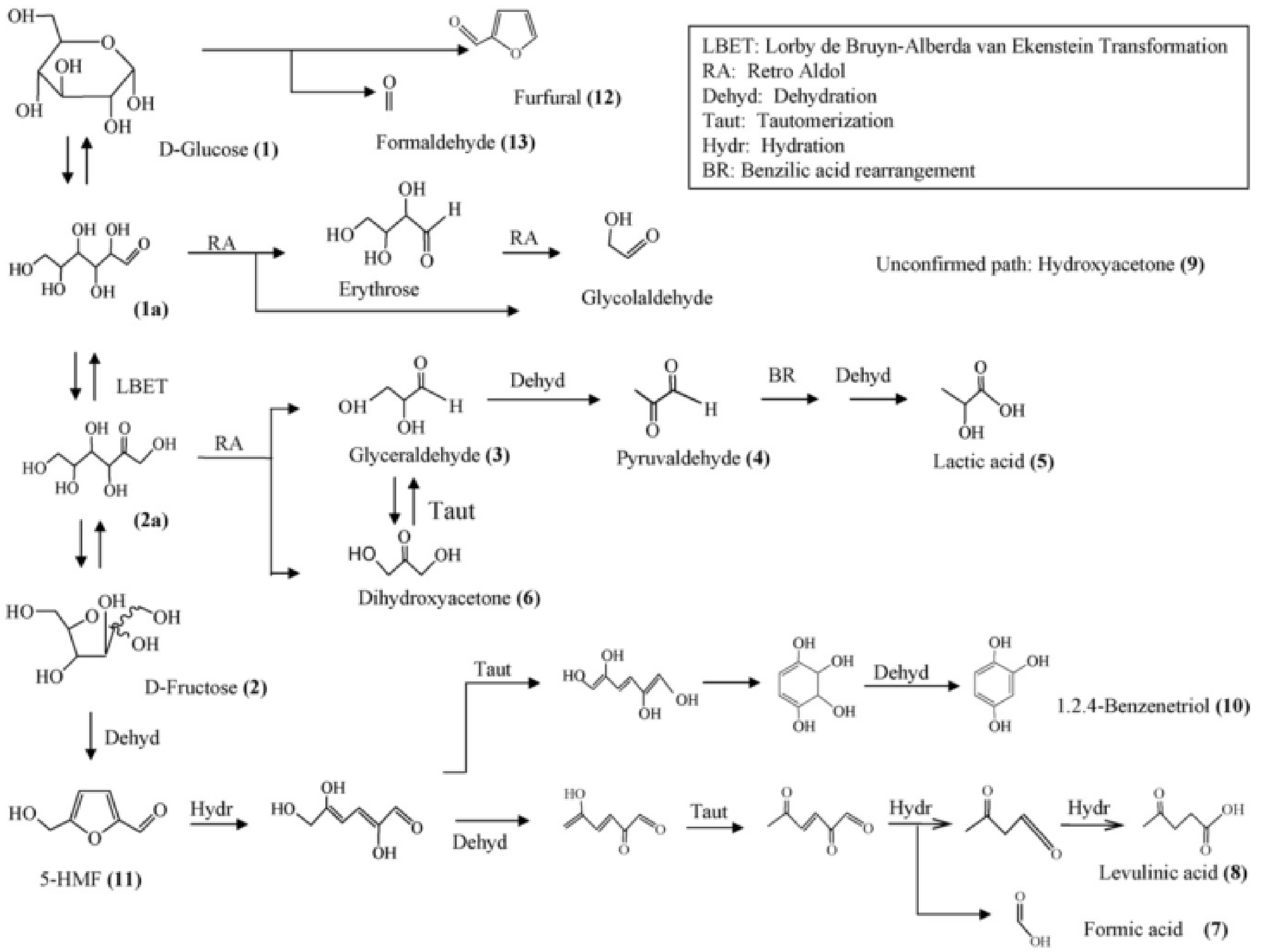

Figure 2.5: Reaction scheme for the gasification of glucose. Adapted from Aida et al. [22]

primary and secondary coke[5]. The primary coke has the shape of the original biomass particle, consists mainly of carbon and has a large internal surface area. Since this report focusses on model components, actual biomass will not be used and this type of coke will play no role in this research. Secondary coke is formed from water-soluble reaction products, which condense to form a tarry material which is converted to coke [5, 26]. This type of secondary coke contains more hetroatoms than primary coke does and it doesn't have any particular shape resembling original biomass or a large surface area.

In literature, it is proposed that 5-HMF plays an important role in the formation of tar [27, 28, 5]. Though it's not the polymerisation of 5-HMF that is leading in tar production, because a glucose feedstock produces char particles 2 orders of magnitude faster than a 5-HMF feedstock does[27]. Char formation is most evident under sub-critical conditions and is believed to form via the mechanism shown in figure 2.8. It was verified by FT-IR and Raman spectrometry that the 5-HMF functional groups were present in the char particles[28].

For the gasification of glucose it was found that a lot of coke was produced during the heat up phase of the experiments [5]. After a 5 minute heat up time, they found that 41.9 % of their 20 wt.% glucose solution had turned to coke, before their 28 ml batch reactor reached 390°C. Thermodynamic calculations have been performed on the coke formation in the gasification of a 100% biomass feed for the theoretical molecule $C_xH_yO_z$[3]. Ternary diagrams which show unavoidable char formation when a 100% biomass stream is gasified are shown in figure 2.9. In the first figure, dots for glucose and sorbitol are shown, indicating that there is little difference between both compounds on a thermodynamic basis and different coking behaviours have to be explained on the basis of intermediate reaction products.

2.4 Influence of pressure on APR

With aqueous phase reforming in a batch reactor, the temperature has a direct influence on the pressure. Therefore pressure and temperature are difficult to evaluate separately. However, literature suggests that the pressure has a minor influence on reactions: For pressures above the critical pressure, its influence on coking tendency is negligible [3]. The formation of some intermediates in gasification reactions is dependent of pressure

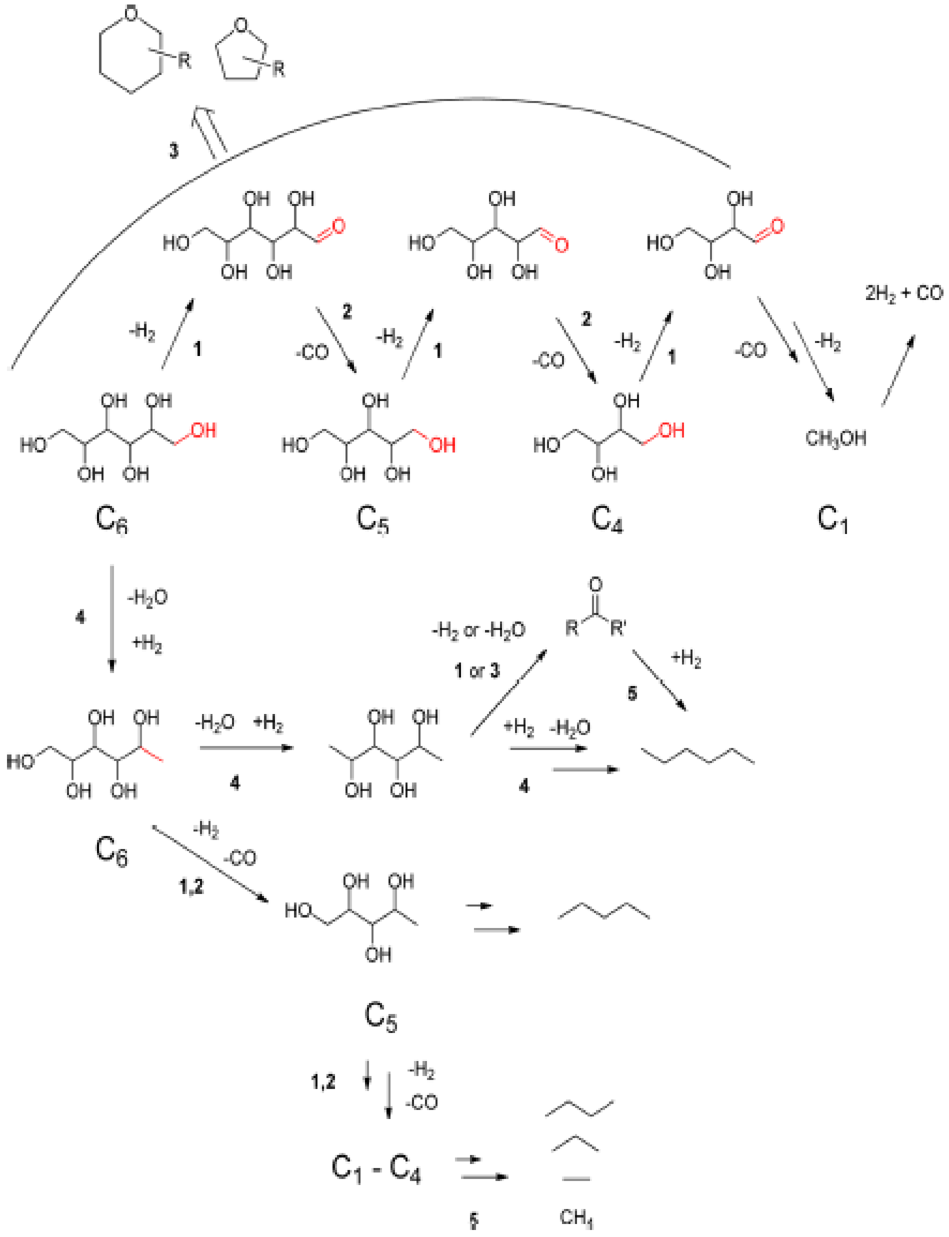

Figure 2.6: Reaction pathways for sorbitol reforming, scheme 1. Adapted from Godina et al. [13]

[17]. When temperatures are high enough for full gasification, the result of this effect on product composition is insignificant [29].

2.5 Infuence of concentration on APR

Concentration is an important factor in gasification experiments. A solution of 1.8 wt.% glucose can be gasified fully, but at higher concentrations a tarry material remains [29]. As concentration increases, the composition of the product gas changes to a smaller hydrogen and larger methane fraction [9]. Reactions to form organic acids, aldehydes and carbonaceous deposits are first order for glucose, whereas reforming reactions are of fractional order, resulting in a decrease in hydrogen yield with increasing concentration [6]. It is mentioned that sorbitol doesn't take side reactions, but no experimental results are there to back this up. It is however expected that sorbitol takes less homogeneous side reaction that glucose [2]. The amount of organic carbon that remains in the liquid phase after reaction decreases with temperature for sorbitol [19].

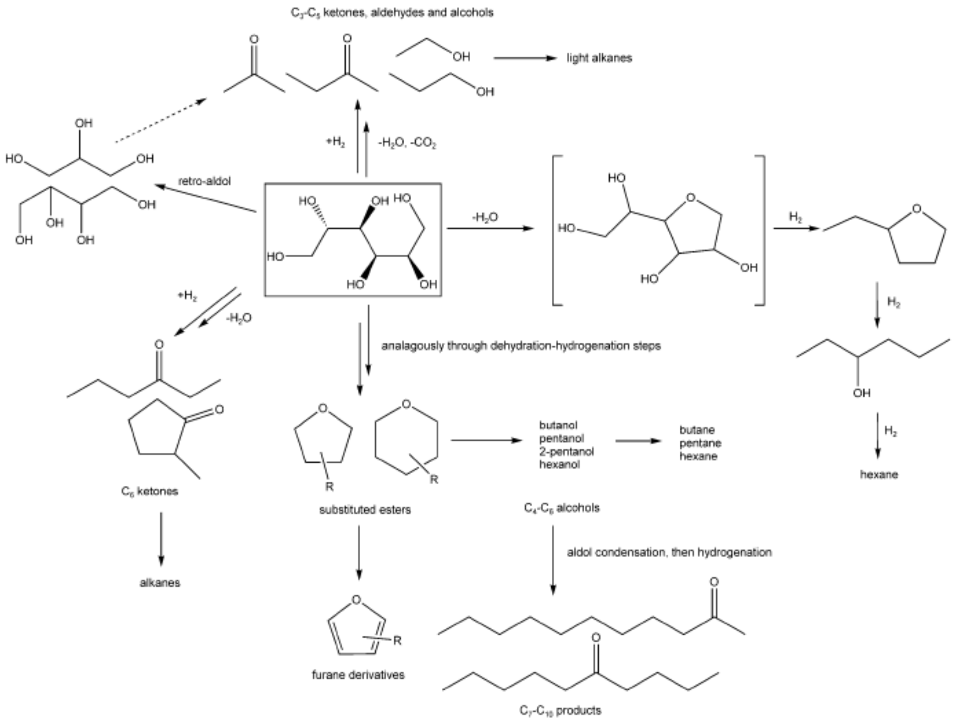

Figure 2.7: Reaction pathways for sorbitol reforming, scheme 2. Adapted from Kirilin et al. [19]

2.6 Influence of catalyst

To gasify biomass at sub-critical temperatures a catalyst is needed [7]. Three types of catalysts: metal, alkali and carbon based, can be used. The alkali and carbon based catalysts are homogeneous and difficult to recover. Therefore the focus is on metal catalysts. It was found that ruthenium catalysts gives high gasification efficiency (70%) in bio-oil conversion, for the same set-up as used in the experiments for this research[30]. Platinum catalyst on the other hand reached 58% efficiency, based on carbon. It was also found that nickel catalyst gave the same gasification efficiency in bio-oil experiments as non-catalytic experiments. Which proves that the reactor set-up (Nickel containing alloy, section 3.1)) and nickel catalyst have the same catalytic efficiency in gasification experiments for bio-oil.

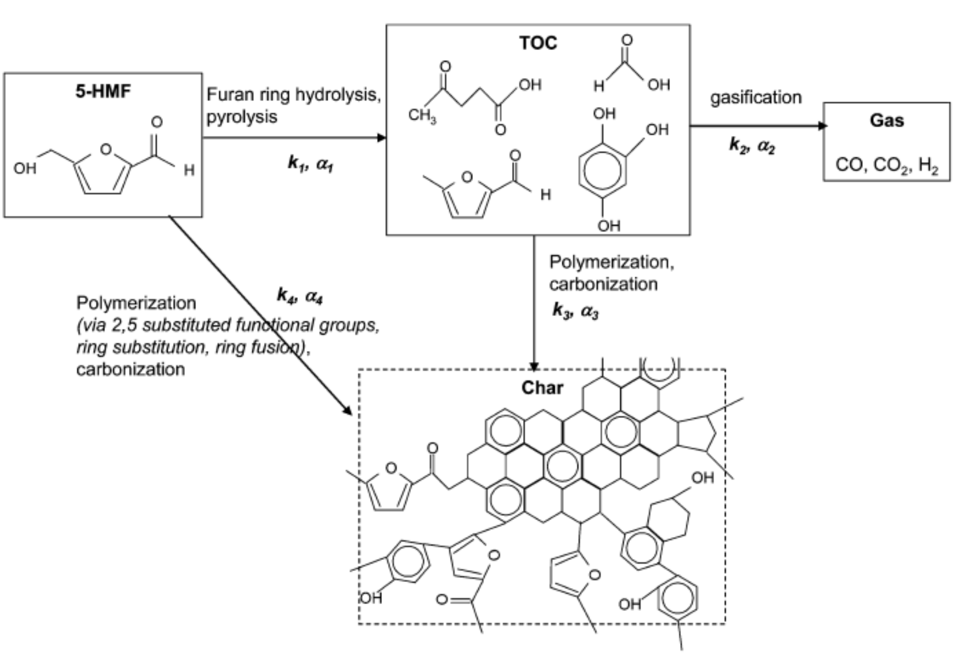

Figure 2.8: Possible reaction pathway for char formation in glucose gasification. Adapted from Chuntanapum et al. [28]

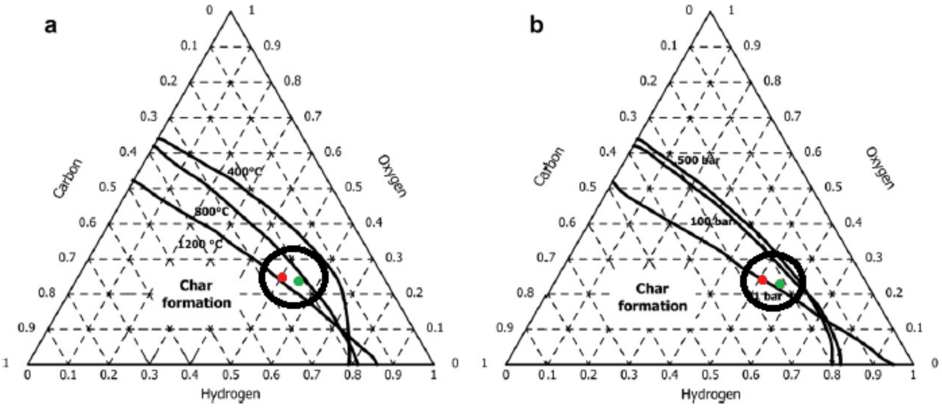

Figure 2.9: Ternary diagram for a generic biomass. Values on the axes refer to the molar ratios of C, H and O in the biomass molecule. (a) Char formation at varying temperature (P = 250 bar); (b) char formation at varying pressure (T = 800 ˚C). Red dot: Glucose, Green dot: Sorbitol. Adapted from Castello et al. [3]

Chapter 3

Practical aspects

3.1 Experimental set-up and materials

Experiments were performed in a 45 ml autoclave batch reactor made of Inconel 600 alloy (∼72% Ni, ∼15% Cr, ∼8% Fe and several other elements). The experimental set-up is shown schematically in figure 3.2. The set-up was placed in a shipping container and controlled from another room, for safety reasons. The set-up contained a fluidised bed and a cooler water bath. The reactor was attached to a pneumatic arm, which allowed the submersion in either the water bath and the fluidised bed. The bed was heated by an oven and the fluidisation gas was pre-heated before entering the bed. Both temperatures could be controlled separately. Different parameters were varied for different goals as shown in table 3.1.

The reactor as seen in figure 3.1 was made up of a tube and a separate top and bottom, which were attached by a conical coupling tightened by a nut and thread on the reactor. The bottom contained an orifice for a temperature sensor and the top had one for a connection to a pressure sensor and gate valve. The reactor was connected to the pneumatic arm by a metal rod. The gate valve was connected to a reducing valve, which could be coupled to a high pressure nitrogen supply or gas volume meter by a removable line. Temperature and pressure data were acquired using Pico Log software. Materials were purchased from Sigma Aldrich. Sorbitol 97% pure and glucose 99% pure.

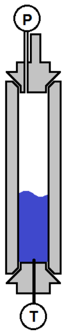

Figure 3.1

Table 3.1: Overview of experiments

Experiment #	**Parameter varied**	**Goal**
1-6	Temperature	Find temperature influence on carbon distribution sorbitol
4-9, 15, 20	Residence time	Find residence time influence on carbon distribution sorbitol
10, 11	Residence time	Find residence time influence on char formation glucose
11, 12	Temperature	Find temperature influence on char formation glucose
10, 11, 13, 14, 17, 23, 24	Sorbitol fraction	Find influence of sorbitol presence on behaviour glucose
18, 19, 21	Temperature	Find temperature at which char formation starts
16, 22	None	Set baseline with pure water

3.2 Experimental procedure

In a typical run, the reactor was cleaned, screw-threads were greased, the vessel was filled with approximately 15 ml feed solution and sealed. Then the reactor was placed in the set-up. To clear the present oxygen from the reactor, it was flushed three times with nitrogen, by pressurising it to 60 barg and subsequent venting to the atmosphere. After that, the reactor was pressurised one more time to 60 barg and the reactor was tested for leaking by leaving it for approximately 5 minutes. If the pressure remained constant, the reactor was deamed leak-free and the pressure was lowered by venting to approximately 30 barg. The oven temperature was set to the desired reaction temperature and the pre-heater to a higher temperature. The difference in temperature of the pre-heater and over varied per temperature setting and per day. The pre-heater was set at such a temperature that the oven could reach its set value and maintain that. This meant a difference of 10-75 ˚C.

To start a measurement, the high pressure room was sealed and from another space, the reactor was lowered into the fluidised bed. Reaction time was defined as the total amount of time that the reactor was in the fluidised bed. This because the initial heat-up was very rapid, but it took a few minutes to bridge the last 20˚C, during which time reactions already take place. After the desired reaction time, the reactor was removed from the fluidised bed and quenched in the cooler water bath, until it reached room temperature. For experiments #1-11 a removable line was connected to a gas burette and the gas present in the reactor was collected there, after which a gas sample was collected. It was not always possible to fit all the gas in the burette. In those cases, the transfer was paused, pressure and volume were noted, some gas was removed and a sample was taken. For the other experiments, #12-24, a gas sample was taken directly from the reactor. Thereafter the reactor was removed from the set-up and opened. The aqueous phase was collected and the reactor was rinsed with

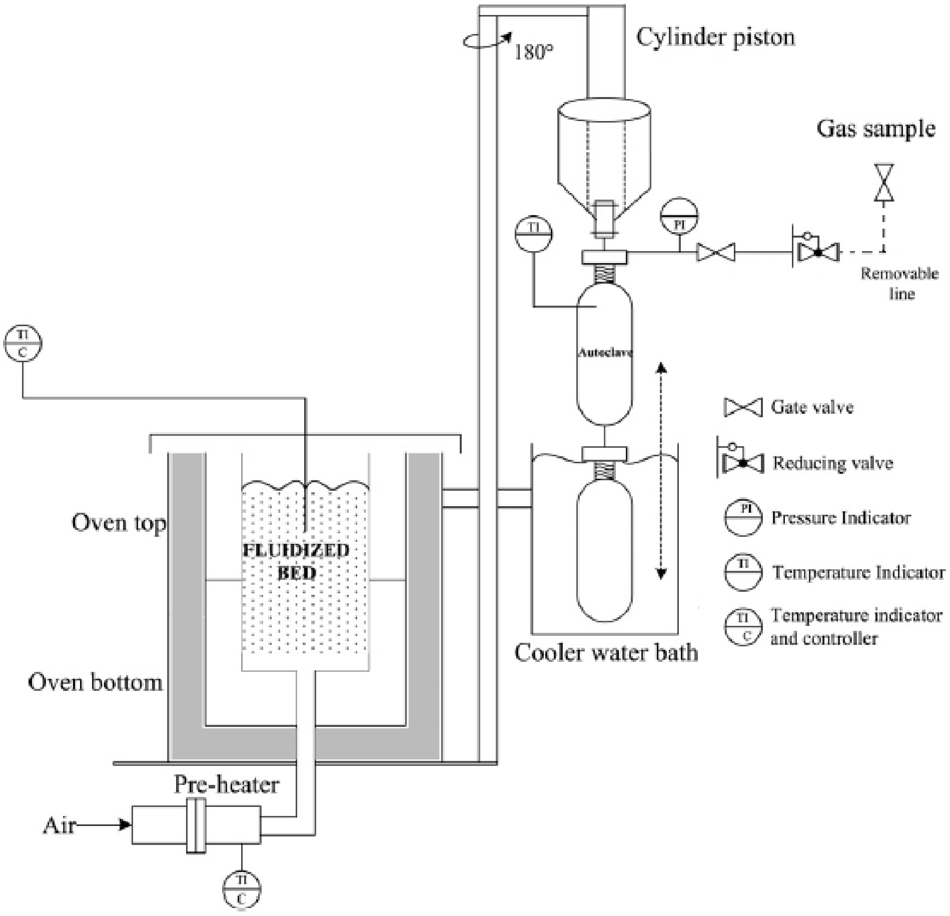

Figure 3.2: Schematic diagram of experimental reactor set-up. Adapted from Chakinala et al. [30]

acetone. The rinsing acetone, including any solids was collected as well. Finally, the reactor was cleaned again. A typical temperature and pressure curve are shown in figures 3.3 and 3.4.

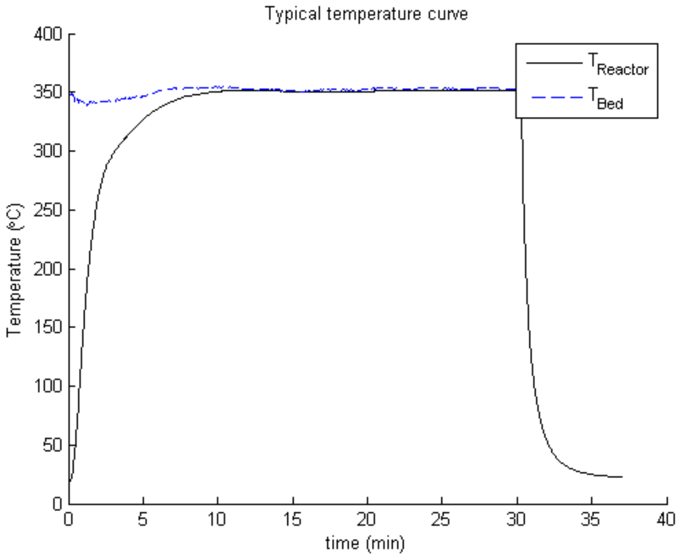

Figure 3.3: Typical temperature behaviour in time (experiment #15).

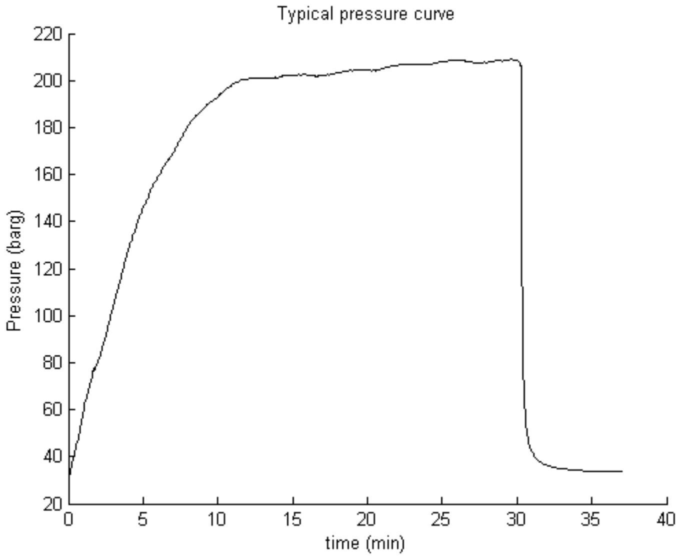

Figure 3.4: Typical pressure behaviour in time (experiment #15).

3.3 Mass and carbon balance measurements and calculations

3.3.1 Mass balance

In preparation for each experiment, a feed solution was made from glucose, sorbitol and water. The masses of glucose, sorbitol and the total amount of solution were measured, as well as the mass of the feed container. After pouring the contents of the container into the reactor, it's weight was measured again. From this, the total amount of feed solution and therefore feed amounts glucose and sorbitol were known.

After reaction, the reactor contained an aqueous phase and for some experiments also oil and char. For each experiment, first the aqueous phase was collected and the reactor was emptied using acetone which was collected separately. If any solids were present, up to experiment #12, these were filtered. When it was found that some solid particles were too small for filtration, in the consecutive experiments, the solids were separated by 30 minutes of centrifugation at 9000 rpm. The oil was dissolved in acetone, which was evaporated by using a rotary evaporator. If any was present in the aqueous phase container, it was separated by decanting the water and drying the oil. Before weighing, solid samples from experiment #1-12 were dried in an over at 150°C. Solids that were in a centrifuge tube were dried at the atmosphere for at least 24 hours.

As mentioned, the gas volume was measured with a gas burette, after which a sample was taken for experiments #1-11. Since a gas burette already contained some atmospheric gas before each measurement, the analysis had to be corrected for this extra initial volume. The sample that was analysed by Micro-GC was representative for the gas initially present in the gas burette and the gas that was released from the reactor until the transfer pause. The total volume that was in the gas burette when the sample was taken is calculated using the oxygen contents of the sample and the following definitions:

V_r = Gas volume flown out of reactor (known).

V_i = Volume of air initially present in gas burette (unknown).

V_b = Total gas volume in gas burette (unknown).

$c_{O_2,air}$ = volume fraction oxygen in air = 0.21 .

$c_{O_2,s}$ = volume fraction oxygen in sample.

The gas from the reactor is diluted by the initial gas. It's not known how much gas was initially there, but since no oxygen is produced in the reaction and the reactor was flushed with nitrogen, it is assumed that all the oxygen in the sample originates from the initial gas. The initial gas has the composition of atmospheric air. The initial volume obeys the relation: $c_{O_2,s} \cdot V_b = c_{O_2,air} \cdot V_i$. This can be expanded and rearranged into: $V_i = \frac{c_{O_2,s}}{c_{O_2,air}} \cdot V_b = \frac{c_{O_2,s}}{c_{O_2,air}} \cdot (V_r + V_i)$. Which results in equation 3.1.

$$V_i = \frac{\frac{c_{O_2,s}}{c_{O_2,air}} V_r}{1 - \frac{c_{O_2,s}}{c_{O_2,air}}} \tag{3.1}$$

The volume of the initial gas was added to the measured volume of gas, which gave the total volume that was analysed. From this the volumes of the gaseous components were calculated and the atmospheric components were subtracted. The remaining volumes were corrected for the volume of gas still in the reactor. It was found that the gas burette didn't give an accurate result, probably due to a leakage during transfer from the set-up to the gas burette. Therefore it was decided to use pressure and temperature data to calculate the volume of gas that would be present at atmospheric pressure. The volumes of gas at 1 atm were calculated using the ideal gas law, for which pressure and temperature were measured and volume occupied in the reactor was calculated at 45 ml minus the volume of the feed solution. It was assumed that a negligible amount gas dissolved in the aqueous phase. Using molecular weights, the mass of the gas was calculated and the total mass of product gas was added to the mass balance to complete it. The amount of nitrogen that was feed to the system was calculated as well, using the ideal gas law and a nitrogen balance was made with nitrogen in and out data. This balance was used to test for a gas leak during the experiment.

3.3.2 Carbon balance

To construct the carbon balance, data from the mass balance was used. With the known feed amounts of sorbitol and glucose and their molecular weight and formula, the amount of carbon that was fed could be calculated. From elemental analysis, the mass percentage of carbon in the aqueous, tarry and solid phases was known. A multiplication with their weights gave the amount of carbon in those phases. The mass of carbon in the gas phase was calculate from the masses of the components, their molecular weight and their molecular formula. If samples for oil and solid phase were to little to analyse, an average value was taken, based on other samples of the same phase and same separation method.

3.4 Analysis methods

For analysis the reaction products were separated and analysed by elemental analysis (EA), Karl Fischer analysis (KF), HPLC, Micro-GC and GC-MS, as shown in figure 3.5.

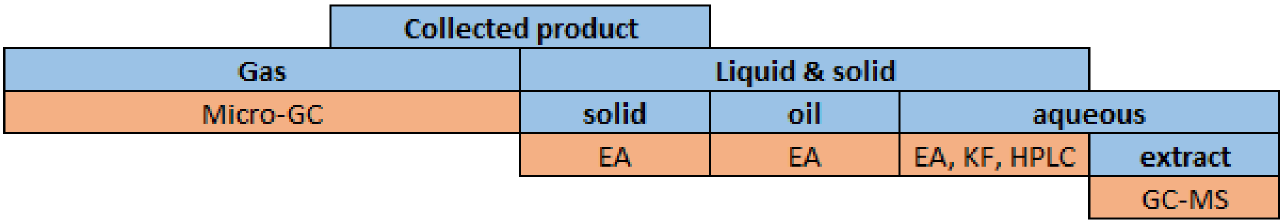

Figure 3.5: Scheme for product analysis, blue: separation, red: analyses

3.4.1 Solid, oil and gas phase analysis

The solid phase was defined as acetone insoluble and it's elemental composition was determined with an elemental analyser (FLASH 2000 CHN Analyzer). Product separation was performed as described in section 3.3, followed by taking a few milligrams of solid and placing it in a tin capsule, which was folded to encapsulate the sample. The oil phase is defined as the water insoluble, but acetone soluble product. The samples were collected as described in section 3.3 and analysed and prepared in the same manner is the solid phase samples. Each product sample was analysed twice and the average value was used in calculations.

Gas phase samples were analysed by micro-GC (Varian CP-4900). The day of analysis, the device was calibrated using calibration gas. Each sample was analysed thrice and the average value was used in calculations. Accuracy was within 5 vol.%.

3.4.2 Aqueous phase analysis

The aqueous phase products were collected as mentioned in section 3.3. They were analysed by several methods. Elemental analysis was performed to give the composition in terms of Carbon, Hydrogen and Nitrogen. Oxygen content was calculated by difference. Samples for EA were prepared by mixing the sample before analysis, pipetting a few micro litres into a tin capsule and sealing it with a press. Each product sample was analysed twice and an average value was used in calculations.

The water content was determined by Karl Fischer titration (Metrohm - 787 KF Titrino 703 TiStand) for the first 6 experiments. The equipment was calibrated before each use with milli-Q water. Samples were weighed on an analytical scale. Each sample was analysed twice and if data weren't conforming with each other, more samples were taken. It was attempted to gain the elemental composition of the dissolved organics by subtraction of water content from elemental analysis data. This was tried for a pure sorbitol solution of known concentration. Elemental analysis data however was not accurate enough to retrieve the elemental composition of sorbitol. Probably to the relatively large inaccuracy in oxygen content, which is calculated by difference from elemental analysis results.

HPLC analysis (Agilent Technologies - 1200 series with VWD and RID or ELSD) was performed on the aqueous phase products to find the amount of unconverted sorbitol or glucose, using a calibration curve for the pure compound. Samples were prepared by diluting the aqueous phase by a factor 10. pH Measurements were attempted, but sample sizes were to little for accurate measurements. For experiment #8, the aqueous phase was extracted with hexane, ethyl-acetate and 1-octanol. The extract was analysed by GC-MS (Agilent Technologies - GC 7890A MS 5975C).

Chapter 4

Results and discussion

Table 4.1: Experimental conditions and balances

Experiment #	1	2	3	4	5	6	7	8	9	10	11	12	13	14	15	16	17	18	19	20	21	22	23	24
T (°C)	150	150	250	250	350	350	350	350	350	250	250	350	250	250	350	350	250	210	235	350	220	350	250	250
Residence time (min)	15	30	15	30	15	30	0	120	15	30	15	30	15	30	30	0	15	0	0	70	0	30	15	15
Sorbitol fraction	1	1	1	1	1	1	1	1	1	0	0	0	0,5	0,5	1	0	0,9	0	0	1	0	0	0,95	0
Wt. % organics	9,99	9,99	10,00	9,97	10,00	9,99	10,00	10,01	9,98	9,93	10,02	10,02	10,00	10,00	10,01	0,00	10,03	10,00	9,75	10,00	9,99	0,00	10,00	0,50
Mass balance closure	0,99	1,00	1,02	1,01	1,02	1,04	1,01	0,98	1,03	0,41	0,99	0,64	0,98	0,79	0,99	0,98	1,03	1,08	0,98	0,99	1,02	0,88	0,97	0,83
Carbon balance closure	1,01	1,02	1,02	1,02	1,01	1,00	1,07	0,91	1,00	1,07	1,14	0,84	1,00	1,00	0,90		1,08	1,09	1,05	0,91	1,06		0,94	1,09
Nitrogen balance closure	1,02	1,03	1,05	1,02	1,10	1,05	1,05	1,02	1,04	1,04	0,98	1,12	1,02	1,04	1,04	1,02	1,03	1,02	1,03	1,00	1,03	0,96	1,02	1,01

All the experiments were performed under the conditions shown in table 4.1. Mass, carbon and nitrogen balances were constructed to determine accuracy of measurements. Experiments with mass balances with an accuracy of ± 10% are defined as reliable. The same goes for carbon balances. The accuracy of the Micro-GC is 5%, therefore an accurate nitrogen balance is defined as ± 5%. It is seen that experiments #10-12, 14, 22 and 24 don't have a good mass or carbon balance. This was due to difficulties with separation for experiments #10,12 and 14. These points were corrected for this, which will be discussed in section 4.4. During experiments #22-24 the reactor was leaking from the bottom, therefore mass data and gas volume data are invalid for those experiments. Only gas phase composition and char formation data were considered reliable data. Experiment #12 is also unreliable in terms of nitrogen balance, therefore gas phase volumes were not used.

4.1 Baseline experiments and P-T relation modelling

In order to be able to see product gas being produced during the reaction, it was attempted to model the pressure dependence on temperature in the autoclave batch reactor. Any extra pressure above the modelled pressure would then be due to produced gas, which would show when gas production started and at what rate. In order to do this, several factors were taken into account:

1. Vapour pressure of water increases with temperature.
2. Pressure exerted by nitrogen increases with temperature.
3. Water expands when heated.
4. Nitrogen may dissolve in water.
5. Dissolved organics may influence the vapour pressure of water.
6. Evaporation of water with increasing temperature reduces liquid water volume

To address factor 1, the vapour pressure of water was calculated using the Antoine equation. The temperature range was separated in two ranges: 255-373 K and 373-747 K, to ensure the validity of the Antoine constants [31, 32]. The available volume for gas molecules was taken as the reactor volume, minus the volume taken by the aqueous phase. It was found that at a temperature of 350 °C, the density of water would have halved, making this expansion significant for the available volume for gas molecules, as mentioned by factor 3. Therefore, data for the temperature dependence of the density of liquid and gaseous water were collected and a second degree polynomial was fitted to both datasets [31]. The respectable volumes of both the liquid (V_l) and vapour phase (V_g) were calculated by temperature dependent density data (vapour density ρ_g Liquid density ρ_l), a mass balance (mass of gas m_g, mass of liquid m_l, total mass m_t) and the reactor volume (Vr). The liquid volume was known from equation 4.3 and that of the gas phase from equation 4.2.

$$m_t = m_g + m_l = \rho_g(T) \cdot V_g(T) + \rho_l(T) \cdot V_l(T) \tag{4.1}$$

$$V_g(T) = V_t - V_l(T) \tag{4.2}$$

$$V_l(T) = \frac{m_t - \rho_g(T) \cdot V_t}{\rho_l(T) - \rho_g(T)} \tag{4.3}$$

Factor 2 was addressed by using the initial pressure, temperature and volume of nitrogen in the system and using the ideal gas law to calculate its pressure at T via: $P_{N_2}(T) = \frac{P_0 \cdot V_g(T_0) \cdot T}{T_0 \cdot V_g(T)}$ It was calculated using temperature dependent Henry's law constants and calculated partial pressure of nitrogen at 350 °C that less than 1% of nitrogen dissolved in the aqueous phase [31]. Therefore dissolution into the aqueous phase was considered negligible. Although sorbitol and glucose could take op 10 % of the solution by mass, the molar concentration is about 1 mole%, therefore it's influence on the vapour pressure of water was negligible.

The total pressure of the system was calculated by adding partial pressures of nitrogen and water. This was plotted versus temperature and shown in figure 4.1. Also in that figure, experimental data from experiments #4,6 and 26 was plotted. # 4 and 6 were 30 minute experiments with sorbitol that yielded almost no gas at 150 °C and 250 °C. Experiment #26 was the heating of pure water to 350 °C for 15 minutes. The experimental heating and cooling are plotted separately. For the modelling, initial nitrogen pressure was taken as 31 bar at 20 °C, with 15 ml of water in the reactor.

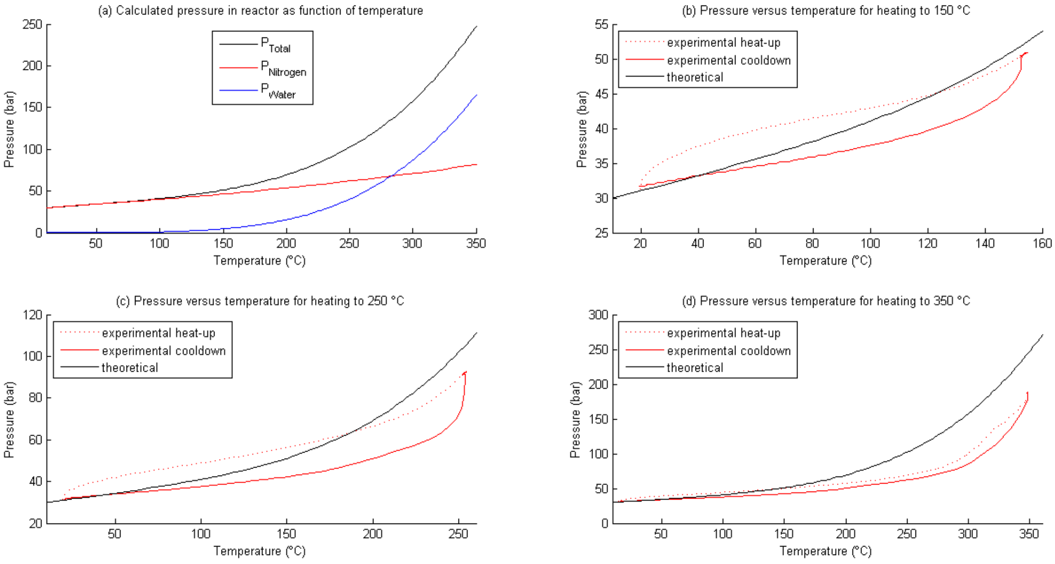

Figure 4.1: Calculated and experimental results for the dependence of pressure on temperature

It can be seen in figure 4.1 b-d that there is a distinct difference in the heating and cooling of the reactor (Less visible at 350 °due to the scale of the Y-axis, but equally large as at 250 °C). This hysteresis is because during the heating up, the pressure is higher than with the cooling. An explanation for this lies in the way in which temperature and pressure are measured. As seen in figure 3.1, the temperature sensor is in the liquid phase and the pressure is measured in the gas phase. When the reactor is submersed in the fluidised bed, the temperature of the reactor changes drastically. It then takes some time to transfer the heat from the reactor wall to the aqueous phase, whereas the gas phase is heated almost instantaneously as is has a much smaller heat capacity, thus it's temperature would be approximately equal to the reactor wall. Basically the temperature sensor is lagging behind the pressure sensor due to resistance to heat transfer. During the quenching, the reverse process takes place, showing a lower pressure than expected based on temperature data. As this cooling is faster than heating it is expected that the difference is larger there. This is confirmed in the 250 °C plot, but is unclear in sub figures b and d.

It is also noted from figure 4.1 that the final pressure that is reached at the maximum temperature is wrongly predicted by the model. It was hypothesised that the reason for this is in the experimental set-up. The pressure sensor is is not located in the hot fluidised bed, but located above it. The reactor is connected via a flexible tube of approximately 30 cm to the pressure sensor. At temperatures above approximately 200 °C, the pressure contribution of water vapour becomes significant and at 280 °its partial pressure is larger than that of nitrogen. The dependence on temperature of the vapour pressure is a lot more steep than that of nitrogen partial pressure. It could be that the vapour in the line connecting the pressure sensor to the reactor is cooler, causing some water to condense and showing a lower pressure. This would on it's turn cause a mass flow of gas to the place where it's condensing due to the pressure difference, resulting in more steam condensing. This hypothesis was in agreement with the fact that after every experiment water was found in the tube connecting the reactor to the pressure sensor.

To verify the hypothesis, an experiment was conducted in which the initial pressure was atmospheric. Results of this experiment were compared to modelled data and are presented in figure 4.2. This shows excellent agreement between the data from Antoine's equation data and experimental data in this set-up. Therefore it is concluded that the difference is not due to water condensation in a cooler zone of the set-up, but it must have to do with the partial nitrogen pressure. As can be seen in figure 4.1a and d, at 348 °C, experimental pressure was found to be 188 bar. At this temperature the vapour pressure of water is approximately 162 bar, this the partial pressure of nitrogen was only 26 bar at 350°C, where it was 30 bar at 20 °C. Possible explanations for this are non-ideal behaviour of nitrogen at these high temperatures or a higher solubility of nitrogen in water than expected on the basis of Henry's law due to changing water properties near the critical region. The first hypothesis could be tested by heating only nitrogen to see if it behaves as ideal. The second hypothesis by heating nitrogen and water, with just enough water to turn all of it to steam at 350 °C. In that case no nitrogen could dissolve in liquid water, as there is none.

It is also seen in figure 4.2 that no hysteresis is seen. This confirms the hypothesis proposed that the gaseous phase is changing in temperature faster than the liquid phase, causing the temperature sensor to lag behind the pressure sensor. That is the case, because the vapour pressure exerted by water is directly dependent on the temperature of the liquid water. Showing that the gaseous nitrogen caused the hysteresis by a faster heating rate. This could further be verified by slowly heating the reactor (including nitrogen and water) ensuring that every part of the reactor has the same temperature. If the hypothesis is true, than the hysteresis should not be visible, because gaseous and liquid phase would have the same temperature.

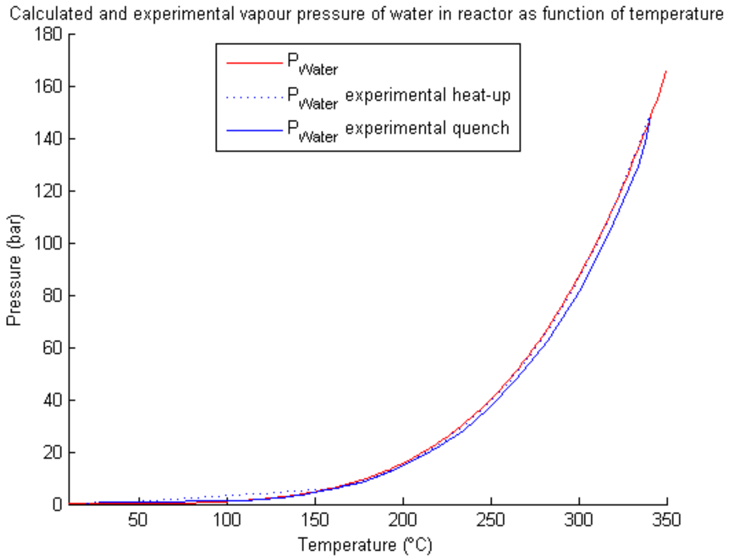

Figure 4.2: Calculated and experimental results for the vapour pressure of water as a function of temperature

4.2 Sorbitol destruction

For sorbitol to be a suitable compound for hydrothermal gasification, it must not take char-producing side reactions at the temperature at which the catalysed gasification reactions take place. Therefore the stability of a sorbitol solution was tested for 15 and 30 minutes residence time, for temperatures of 150 °C, 250 °C and 350 °C, as shown in figure 4.3. It is seen that at 150 °C, no sorbitol is converted and that at 250 °C, 3 % of the sorbitol is converted. That 3 % difference measured is significant, as can be seen by the accuracy of the calibration curve in appendix A. At 150 °C and 250 °C, the residence time is of insignificant influence on the sorbitol destruction. At 350 °C, duplo measurements show good agreement and show that at this temperature more than 90% of sorbitol is converted. It is also noted that a longer residence time increases sorbitol destruction, as will be discusses in section 4.3.1.

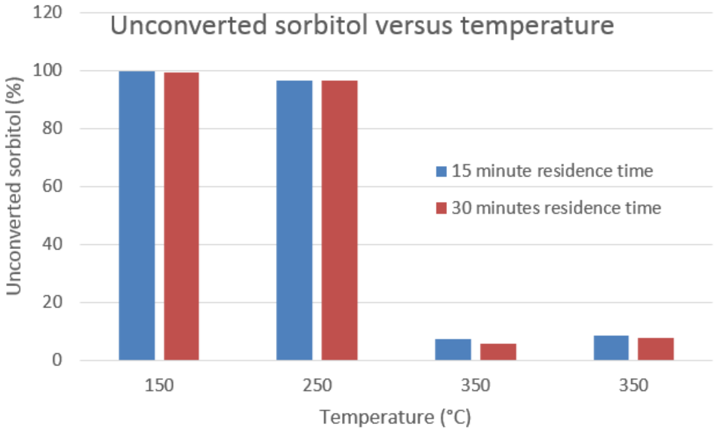

Figure 4.3: Mass percentage of sorbitol that remained unconverted for various temperatures at 15 and 30 minutes residence time.

4.3 Carbon distribution sorbitol experiments

4.3.1 Aqueous and oil phase

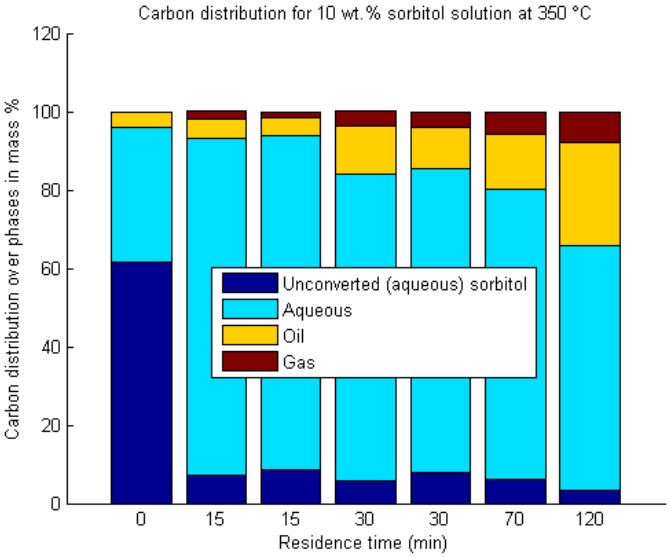

Figure 4.4: Carbon distribution amongst phases and sorbitol destruction for various residence times at 350°C

Figure 4.4 shows the carbon distribution as mass % for experiments with only sorbitol solution as feed. The temperature of the reaction was kept at 350°C. The first measurement shows a 0 minutes residence time. In that experiment the reactor was heated to 350°C and immediately quenched. Several trend can be seen in the figure.

The first thing that is visual is that during the heat-up of the reactor, roughly 40% of the sorbitol feed is converted already and that after 15 minutes less than 10% is left. It's also visible that even after 120 minutes residence time, not all the sorbitol is converted. A possible explanation for this is that at 350°C, a rapid equilibrium (within 15 minutes) is reached between sorbitol and one or more of it's degradation product. Then as the reaction proceeds, that degradation product slowly reacts further, shifting the equilibrium to less sorbitol.

It is also noted that the amount of carbon present as oil, increases with time. The oil produced was always a very thick oil. It wasn't runny at room temperature. Carbon contents was between 60-75 wt.% for most samples. As the oil formation causes the amount of aqueous carbon to decrease, it is obvious that the oil is a polymerisation product of one or more of the degradation products of sorbitol. Also noted from figure 4.4 is that both 30 minute experiments show comparable composition, where one has a carbon closure of 100% and another only 90 %, indicating that a 10% difference in carbon closure does not necessarily compromise on accuracy.

4.3.2 Gas phase

The amount of carbon that goes into the gas phase also increases with residence time. Figure 4.5 shows the total gas production in mole per mole sorbitol fed. The top image shows the entire plot and the bottom is zoomed in. It is seen that the amount of each type of gas increases, but that the amount of C_2H_6 is equal for 70 and 120 minutes residence time.

As can be seen, the production of C_3H_6 is visible after 15 minutes and the production of C_2H_4 after 30 minutes. It is possible that those products occur due to the acid catalysed elimination of the alcohol group from respectively propanol or ethanol. The pH of the aqueous phase was tested with pH paper, which showed a pH of approximately 2.5, possibly favouring the conditions for that reaction. this is in agreement with the reaction path outlined in figure 2.7. From this it's also proposed that C_3 alcohols are formed earlier in the degradation process than C_2 alcohols. This might be due to the $C6$ chain splitting into two C_3 glycerol chains as described in figure 2.7. Elimination of CO_2 and H_2O may than produce C_2 chains.

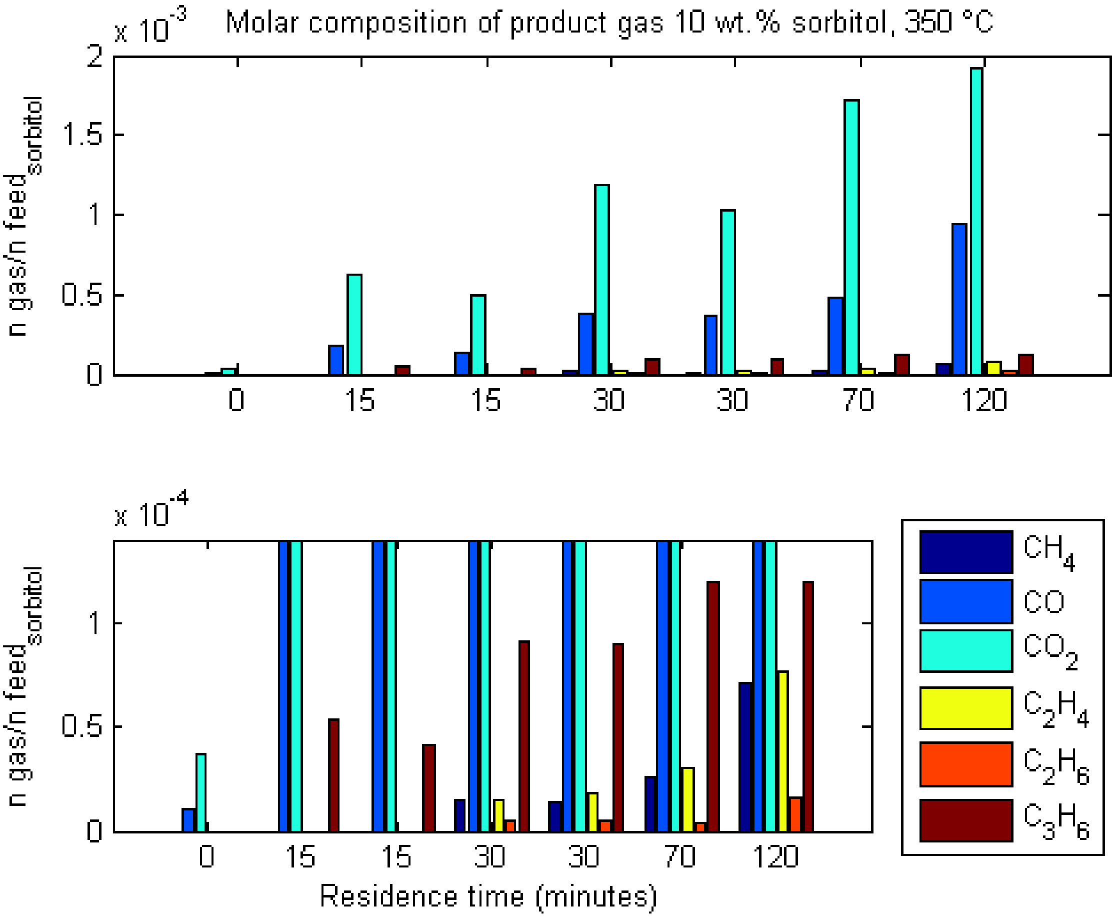

Figure 4.5: Gas production in mole per mole sorbitol fed for different residence times at 350°C reaction temperature.

Another interesting fact that was noted during the reaction is that the pressure starts to slowly decline after 50-60 minutes of reaction time. As shown in figure 4.6 the pressure increases during the first part of the reaction

Table 4.2: Moles of CO per mole of CH_4 for various residence times for 10 wt.% sorbitol experiments at 350 °C

Residence time (minutes)	$\frac{n_{CO}}{n_{CH_4}}$
30	25.0
30	26.6
70	18.8
120	13.3

but later drops, whereas the temperature remains constant (Solid red line. The dashed red line shows drops in the pressure curve due to temperature changes of fluidised bed and reactor). This was at first visible for experiment #8 and was retested in experiment #25 (not mentioned in table 4.1, because only gas phase analysis was performed. Dashed red line in figure 4.6) The nitrogen balance of experiment #8 closed, confirming no leakage, just as that of experiment #20 (70 minutes residence time). Unfortunately a power shortage caused half of the experimental data of experiment #20 to be lost and the nitrogen balance of experiment #25 only closed to 93%, showing a leak. This is also visible in the graph as the pressure difference between the two experiments increases with time. The pressure drop without leaking cannot be explained by the water-gas shift reaction, equation 2.1, since the number of non-water gas molecules remains constant and partial pressure of water is based on it's vapour pressure. The pressure drop might be caused by the methanation of CO as described in equation 2.2. This reduces the total number of non-water gas molecules and thus pressure.

To verify the aforementioned hypothesis, the molar amount of carbon monoxide was compared to that of methane and is was found that the relative amount of carbon monoxide decreased, as shown in table 4.2, which is in agreement with the hypothesis. However, the amount of methane produced is only 0.07 mmole, which could account for approximately 0.5 bar in pressure loss. Therefore, something else must be happening. It is possible that other types of hydrogenation take place, for instance the hydrogenation of double carbon-carbon bonds present in some aqueous phase products, as proposed in figures 2.6 and 2.7. This could be verified by performing aqueous phase analysis as described in section 3.4 on samples from different residence times, in a quantitative manner. It can then be determined if at the time that the pressure starts declining, hydrogenation takes place. A more easy method for that would be to use a Micro-GC that can detect hydrogen and see if that is disappearing it some residence time. If this is also not the case, it might even by that the reactions cause the aqueous phase properties to change, allowing more gas to dissolve in it.

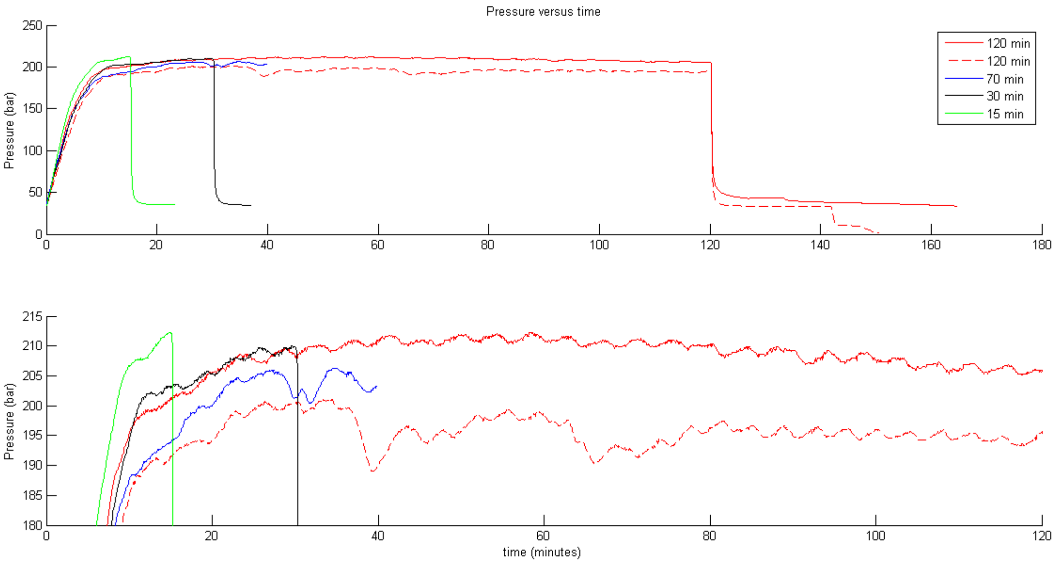

Figure 4.6: Pressure as function of temperature for 10 wt.% sorbitol experiments as 350°C.

4.4 Char production

It was found that sorbitol on it's own only produced oil and no char. Glucose on the other hand definitely produces char, as can be seen in figure 4.7. After 30 minute of residence time, almost 80% of the carbon is in the solid phase as char. In beginning of the chapter, it was mentioned that experiment #10 had an incomplete mass balance. This was due to the nature of the char produced, which was very voluminous and was stuck to the reactor. A lot of water adhered to the char and was later rinsed with acetone. To solve this, it was assumed that all carbon in the aqueous phase was less volatile than water. The mass balance was then solved to be 1, by changing the mass of aqueous phase. This caused the carbon balance to increase, because this was calculated using the mass of aqueous phase and it's concentration. This increase in aqueous carbon was subtracted from the solid phase carbon, to prevent from counting it twice. The result was a carbon balance of 107% closure, which is acceptable.

4.4.1 Temperature of char formation

To determine at which temperature the formation of char started, experiments were conducted in which a glucose solution was heated to a certain temperature. Since the residence time was very brief, amounts of char produced were in the order of tens of milligrams, which wouldn't result in an accurate carbon balance. Therefore results are presented in table 4.3. It is seen that char formation already occurs at 210 °C, the lowest temperature used in glucose experiments. It is also seen that no char is produced at 220 °C. It might be possible that the heating rate has an influence in the char formation mechanism. During experiment #21, the heating rate was higher than in experiment #18. The latter has spent a total of 125 seconds at a temperature above 200°C to be heated to 210°C, whereas experiment #21 has only been above 200°C for 91 seconds as seen in table 4.3.

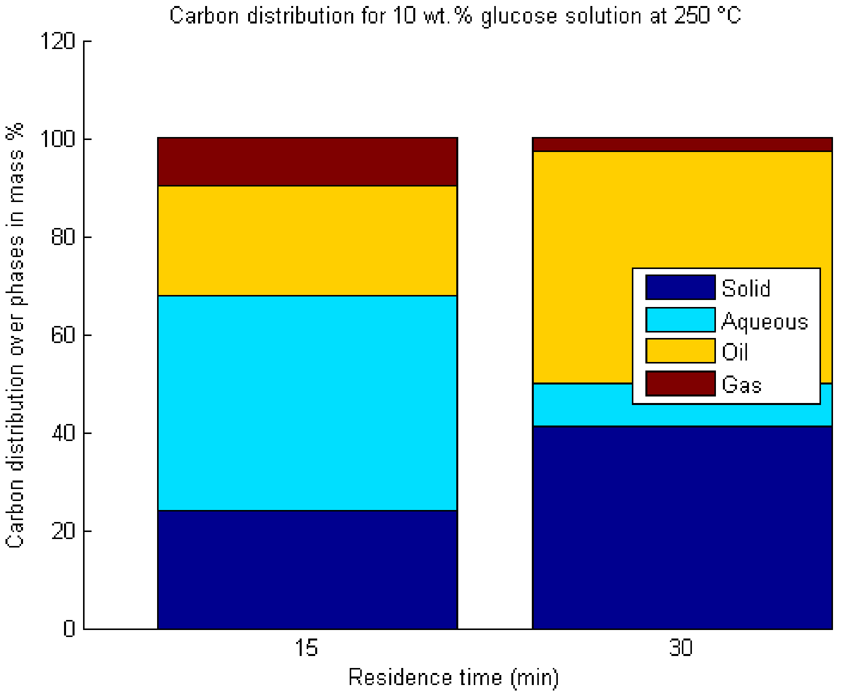

Figure 4.7: Carbon distribution amongst phases for glucose at various residence times at 250°C

Table 4.3: Char formation in 10wt.% glucose heat-up experiments

Experiment #	18	21	19
T (°C)	210	220	235
Char formation	yes	no	yes
Time above 200 °C (s)	125	90	183

4.4.2 Influence of glucose fraction on char formation

Due to the complex char formation mechanism described in section 2.3, via 5-HMF as the backbone for char production and various other components being attached to it, it could well be that some degradation products of sorbitol were to be converted to char. It was found that the amount of char produced, when the organic feedstock contained equal amounts of glucose and sorbitol, the char formation more than halved, as can be seen in figure 4.8. It is also noted that at glucose fractions of 0.1 and 0.05, the fraction of carbon to char is increasing again. However, respective masses of char found were 20 and 14.6 milligrams. The char mass of the 0.1 glucose fraction was measured at a scale with an accuracy of 10 mg, resulting in more than 50 % error. The other sample was weighed more accurately, but still the error would be around 10% (assuming 1 mg error in scale and additional error in elemental analysis).

From the data at 1 and 0.5 weight fractions of glucose it can be concluded that at 10 wt. % total organics, a lower glucose fraction results in less carbon fed as glucose to char. However, this doesn't not say anything about a possible interaction between glucose and sorbitol. The effect seen could be solely due to the lowering of the total concentration of glucose in water or be influenced by sorbitol presence. To verify the influence of sorbitol presence, experiments should be repeated with the same concentration of glucose, but without sorbitol. In this research this was only done for 0.5 wt. % glucose. Unfortunately a leak in the reactor during the reaction caused mass data to be totally unreliable. It was however found that char was produced. Therefore is can be concluded that even at 0.5 wt.% glucose, char formation occurs, although it was found in literature that at supercritical conditions 1.8 wt.% could be gasified fully [29]. This means that heating-up rate could have a drastic effect on char formation, as glucose is unstable and prone to form char under sub-critical conditions at 250 °C, even in low concentration of 0.5 wt.% .

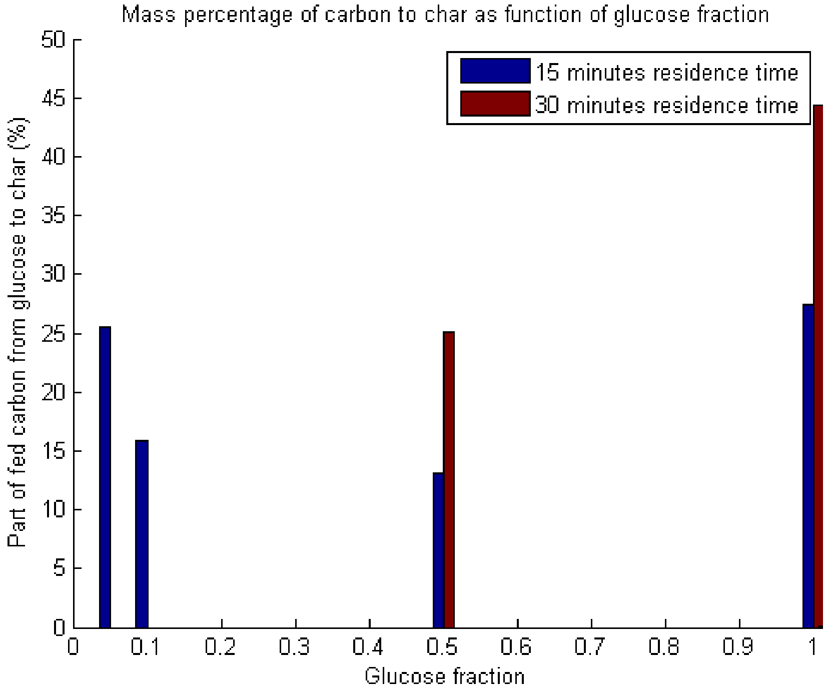

Figure 4.8: Influence of glucose fraction on mass of carbon recovered ass char is percentage of carbon fed is glucose, for 10 wt.% total organics at 250 °C

4.4.3 Structure and composition of char

The composition of char was found to be relatively constant throughout the experiments, but dependent on separation techniques, with values ranging between 60-70 wt. % carbon for filtered samples and ~ 50 wt. % carbon for centrifuged samples, as seen in table 4.4. The difference in carbon content is probably due to the fact that all water is removed by filtration, as the residue is washed with acetone and dried in an oven, whereas centrifuged samples were dried at the air, not removing all water. Therefore, the carbon content of pure char should be an average of experimental data from experiments #10-14, thus 66 wt. % carbon. For carbon balances this difference is of no influence as mass of solid phase and carbon fraction are both dependent on water content.

The particle size was found to be dependent on temperature, in such a way that the longer the residence time, the larger the char particles became. In the experiments up to 15 minutes of residence time, most of the char particles were to small to be filtered by a five micron filter. As mentioned in section 3.3, char particles from those residence time experiments were separated by centrifugation at 9000 rpm for 30 minutes. In the 30 minute experiments however, a large mass fraction of the total amount of char could be filtered and a minor amount had to be centrifuged.

Table 4.4: Carbon and hydrogen content for solid samples

Sample #	Average carbon content (wt. %)	Average hydrogen content (wt. %)
11	65,5%	4,2%
12	71,3%	3,5%
13	61,5%	5,0%
14	65,3%	4,2%
10	66,4%	4,4%
17	47,7%	6,3%
18	48,8%	5,9%
23	52,0%	6,5%

4.5 Aqueous phase analysis for sorbitol experiments

Samples of the aqueous phase of experiment #8 were qualitatively extracted with hexane, ethyl acetate and 1-octanol to test the best solvent to extract the aqueous phase with for GC-MS analysis. It was found that hexane and ethyl acetate are good solvents for extraction. In both solvents various components were found, which are summarised in table 4.9. Some components were found in each of the solvents: Isosorbide, acetic acid, furans. Others were only found in one of the solvents. Octanol proved to be a bad solvent for extraction, since it didn't yield as much compounds as the other solvents and few unique results, as can be seen in appendix B.

One of the most significant components (area percentage wise in the GC-MS spectrum) was isosorbide, the product of the double dehydration of sorbitol. This component is neither mentioned in the reaction paths outlined in figure 2.6, nor in that of figure 2.7, but was found in the master thesis of M. van Lotringen [33]. However, the second figure as proposed by Kirilin et al. does show the product of the single dehydration of sorbitol and mentions it only reacting with hydrogen. If properties of isosorbide make is relatively stable, it could be that this is the product with which sorbitol is in equilibrium with as proposed in section 4.3.1. Acetic acid, which was also found in all extraction solvents, isn't mentioned in either one of the proposed reaction paths either. However, the authors of the reaction scheme mention that they found acetic and propanoic acid [19] and propose their formation by dehydrogenation/oxidation of alcohols. Also the furans are mentioned in the reaction scheme of figure 2.7.

The catalyst used by Kirilin et al. was Pt/Al_2O_3 and their reactor was stainless steel. Like Inconel 600 alloy used for the reactor in the experiments in this work, stainless steel alloy contains significant amounts of chromium and nickel. Unfortunately Kirilin et al. didn't publish any non-catalytic results, but the catalytic activity of nickel is well known and could explain similarities in reaction products [17]. To verify this, an experiment under the same conditions should be performed in a reactor that isn't catalytically active, for instance a glass reactor.

Component	**Structure**	**Component**	**Structure**
Acetic Acid	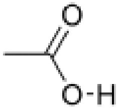	Cyclopentanone	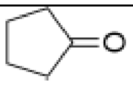
Acetol	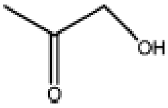	2-furaldehyde	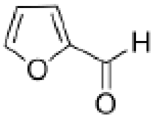
methyl-furan		1-(2-furanyl) ethanone	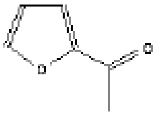
Pentanoic acid	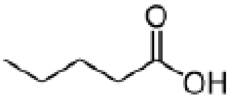	3-methyl-2-cyclopenten-1-one	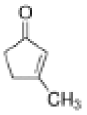
Isosorbide	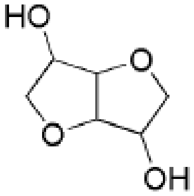	Acetone	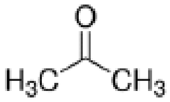
3-methoxyphenol	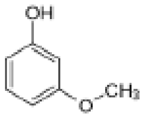	1-hexanol	
n-propyl acetate	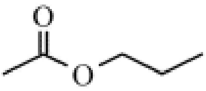	Phenol	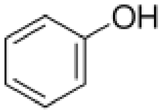
3-pentanone	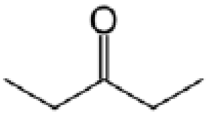	Propanoic acid	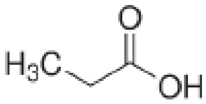

Figure 4.9: Reaction products found in Aqueous phase by extraction followed by GC-MS for 10 wt.% sorbitol at 350 ˚C for 120 minutes

Chapter 5

Conclusion

An experimental procedure and scheme for analysis have been made to ensure reliable results for experiments. Gas samples should be taken directly from the experimental set-up and calculations on the amount of gas should be based on pressure and temperature data. A scheme for analysis is presented in figure 3.5. Solid samples should be filtered, washed and dried in an oven if composition is to be measured and for carbon balance closure, centrifugation is the best separation method.

A model has been made for the dependence of pressure in this reactor on temperature. Experimental data didn't show agreement with the model above temperatures of 150 ˚C, which was proven to be due to partial pressure of nitrogen. It is hypothesised that a substantial amount of nitrogen is absorbed in hot compressed water, due to property changes of water in the sub-critical region near the critical point.

In sorbitol experiments it was found that below 250 ˚C sorbitol is stable for at least 30 minutes residence time. It was also found that oil and gas production increase with residence time at 350 ˚C. Sorbitol destruction at 350 ˚C is 40 % during the heat-up period and more than 90 % after 15 minutes. For longer residence times the amount of destructed sorbitol slowly increases, but doesn't reach full destruction within 120 minutes, implying some sort of rapidly formed equilibrium between sorbitol and one of it's degradation products.

Gaseous product formation also increases with temperature. Carbon dioxide and monoxide start to from during the heat-up phase, as is seen in figure 4.5. Within 15 minutes propylene production is measured and ethylene and methane production are noticed within 30 minutes. Pressure start to drop after 50 minutes of reaction time, possibly due to methanation of CO. Propylene and ethylene are possibly formed by dehydration of propanol and ethanol.

Char formation for 10 wt.% glucose solution was found at a temperature of 210 ˚C and is probably dependent on heating rate, where a faster heating rate, thus less time at elevated temperature would reduce the char formation tendency. Char and oil production increased with temperature and after 30 minutes at 250˚C, 41 wt.% is present as char and 47 wt.% as oil. Even in dilute solutions of 0.5 wt.% glucose, char is formed at 250 ˚C. Influence of sorbitol presence on char formation has not been ruled out nor confirmed. Carbon contents of char and oil is similar, with char having a carbon mass percentage between 60-70 wt.% and oil between 60-75 wt.%. Char particle sizes increase with temperature and th smallest particles at 15 minutes residence time are smaller than five micron.

Analyis of aqueous phase components for experiment #6 showed agreement with the reaction paths presented in figure 2.7. It was found that hexane and ethyl acetate are good solvents for extraction, but octanol isn't. Acetic and propanoic acid were found and acidity was confirmed with pH paper. Isosorbide was identified as a reaction product of sorbitol, unmentioned by reaction schemes.

In regard to the larger goal of making a two stage reaction, with stabilisation of biomass as a first step and gasification as a second, this research proved that sorbitol, a model component for stabilised biomass, does not form char or oil after half an hour at 250 ˚C. Catalytically, sorbitol can however be selectively converted at this temperature[19, 13, 25]. Therefore under optimal conditions and full hydrogenation of biomass (glucose), the principle of the two stage gasification should work. The next steps towards a functional two stage set-up would be stabilisation of real biomass and the catalytic gasification of stabilised biomass or sorbitol.

Chapter 6

Recommendations

Since this is new research a lot of recommendations are made because of the results found in this research. It is recommended that nitrogen absorption in water at 350 °C is further researched to complete the model for the temperature dependence of pressure in this set-up. Once the model shows good agreement, experimental pressure data can be compensated for nitrogen and water vapour pressure. From that data, gas production can be visualised and in combination with gas samples at different times, reactions producing gas can be mapped.

It is also recommended that the influence of the presence of sorbitol on glucose gasification and char formation is further investigated by gasifying glucose at different concentrations at 250 °C and comparing that data with data from figure 4.8. If data are the same, then sorbitol is of no influence and if data differ, sorbitol has an effect on char formation. In those cases it is important that char is separated by filtration, washed with acetone and centrifuged to separate the acetone and to measure only the amount of char produced.

To confirm or deny reaction paths and times at which reactions occur, aqueous phase samples of sorbitol's reaction product for different residence times should be extracted with hexane and ethyl acetate. For that a procedure should be made that allows for quantitative results. Then from those results, relative concentration profiles can be made, showing which compounds react when. Another possibility would be to analyse the aqueous phases with LC-MS. Char and oil should be analysed by FT-IR to yield functional groups in it, giving a clue to which components react to form char.

Chapter 7

Acknowledgement

First and foremost I would like to thank Varsha Paida for helping me with this project, her great suggestions for improvements and pleasant company. Secondly I would like to thank Wim Brilman for the fruitful meetings that gave new insights into topics of investigation. Finally I would like to thank the entire SPT group for their alacrity to help with any problem encountered in the lab and the friendly working environment.

Bibliography

[1] M. S. Dresselhaus and I. L. Thomas. Alternative energy technologies. *Nature*, 414(6861):332–337, 2001. ISSN 0028-0836. doi: 10.1038/35104599. 10.1038/35104599.

[2] Yi Wei, Hanwu Lei, Yupeng Liu, Lu Wang, Lei Zhu, Xuesong Zhang, Gayatri Yadavalli, Birgitte Ahring, and Shulin Chen. Renewable hydrogen produced from different renewable feedstock by aqueous-phase reforming process. *Journal of Sustainable Bioenergy Systems*, 2014, 2014. ISSN 2165-4018. doi: 10.4236/jsbs.2014.42011.

[3] Daniele Castello and Luca Fiori. Supercritical water gasification of biomass: Thermodynamic constraints. *Bioresource Technology*, 102(16):7574–7582, 2011. ISSN 0960-8524. doi: 10.1016/j.biortech.2011.05.017.

[4] Peter McKendry. Energy production from biomass (part 1): overview of biomass. *Bioresource Technology*, 83(1):37–46, 2002. ISSN 0960-8524. doi: 10.1016/S0960-8524(01)00118-3.

[5] Johannes B. Müller and Frederic Vogel. Tar and coke formation during hydrothermal processing of glycerol and glucose. influence of temperature, residence time and feed concentration. *The Journal of Supercritical Fluids*, 70(0):126–136, 2012. ISSN 0896-8446. doi: 10.1016/j.supflu.2012.06.016.

[6] Rupali R. Davda and James A. Dumesic. Renewable hydrogen by aqueous-phase reforming of glucose. *Chemical Communications*, (1):36–37, 2004. ISSN 1359-7345. doi: 10.1039/B310152E.

[7] Prabir Basu. Chapter 7 - hydrothermal gasification of biomass. In Prabir Basu, editor, *Biomass Gasification and Pyrolysis*, chapter Chapter 5 - Supercritical fluids, pages 229 – 267. Academic Press, Boston, 2010. ISBN 978-0-12-374988-8. doi: 10.1016/B978-0-12-374988-8.00007-6.

[8] Falk Harnisch Maria Mller, Peter Nilges and Uwe Schrder. Subcritical water as reaction environment: Fundamentals of hydrothermal biomass transformation. *ChemSusChem*, 4(5):566–579, 2011. ISSN 1864-564X. doi: 10.1002/cssc.201000341.

[9] Ratna F. Susanti, Laras W. Dianningrum, Taewoo Yum, Yunje Kim, Byung Gwon Lee, and Jaehoon Kim. High-yield hydrogen production from glucose by supercritical water gasification without added catalyst. *International Journal of Hydrogen Energy*, 37(16):11677–11690, 2012. ISSN 0360-3199. doi: 10.1016/j.ijhydene.2012.05.087.

[10] Yukihiko Matsumura, Tomoaki Minowa, Biljana Potic, Sascha R.A. Kersten, Wolter Prins, Willibrordus P.M. van Swaaij, Bert van de Beld, Douglas C. Elliott, Gary G. Neuenschwander, Andrea Kruse, and Michael Jerry Antal Jr. Biomass gasification in near- and super-critical water: Status and prospects. *Biomass and Bioenergy*, 29(4):269 – 292, 2005. ISSN 0961-9534. doi: 10.1016/j.biombioe.2005.04.006.

[11] Jrgen O. Metzger. Production of liquid hydrocarbons from biomass. *Angewandte Chemie International Edition*, 45(5):696–698, 2006. ISSN 1521-3773. doi: 10.1002/anie.200502895.

[12] Anand G. Chakinala, Shushil Kumar, Andrea Kruse, Sascha R. A. Kersten, Wim P. M. van Swaaij, and D. W. F. Brilman. Supercritical water gasification of organic acids and alcohols: The effect of chain length. *The Journal of Supercritical Fluids*, 74(0):8–21, 2013. ISSN 0896-8446. doi: 10.1016/j.supflu.2012.11.013. (Wim).

[13] Lidia I. Godina, Alexey V. Kirilin, Anton V. Tokarev, and Dmitry Yu Murzin. Aqueous phase reforming of industrially relevant sugar alcohols with different chiralities. *ACS Catalysis*, pages 2989–3005, 2015. doi: 10.1021/cs501894e.

[14] Ratna F. Susanti, Laras W. Dianningrum, Taewoo Yum, Yunje Kim, Youn-Woo Lee, and Jaehoon Kim. High-yield hydrogen production by supercritical water gasification of various feedstocks: Alcohols, glucose, glycerol and long-chain alkanes. *Chemical Engineering Research and Design*, 92(10):1834–1844, 2014. ISSN 0263-8762. doi: http://dx.doi.org/10.1016/j.cherd.2014.01.003.

[15] In-Gu Lee, Mi-Sun Kim, and Son-Ki Ihm. Gasification of glucose in supercritical water. *Industrial & Engineering Chemistry Research*, 41(5):1182–1188, 2002. ISSN 0888-5885. doi: 10.1021/ie010066i.

[16] Sascha R. A. Kersten, Biljana Potic, Wolter Prins, and Wim P. M. Van Swaaij. Gasification of model compounds and wood in hot compressed water. *Industrial & Engineering Chemistry Research*, 45(12): 4169–4177, 2006. ISSN 0888-5885. doi: 10.1021/ie0509490.

[17] R. R. Davda, J. W. Shabaker, G. W. Huber, R. D. Cortright, and J. A. Dumesic. A review of catalytic issues and process conditions for renewable hydrogen and alkanes by aqueous-phase reforming of oxygenated hydrocarbons over supported metal catalysts. *Applied Catalysis B: Environmental*, 56(12):171–186, 2005. ISSN 0926-3373. doi: 10.1016/j.apcatb.2004.04.027.

[18] R. D. Cortright, R. R. Davda, and J. A. Dumesic. Hydrogen from catalytic reforming of biomass-derived hydrocarbons in liquid water. *Nature*, 418(6901):964–967, 2002. ISSN 0028-0836. doi: 10.1038/nature01009. 10.1038/nature01009.

[19] AlexeyV Kirilin, AntonV Tokarev, ElenaV Murzina, LeonidM Kustov, Jyri-Pekka Mikkola, and DmitryYu Murzin. Reaction products and transformations of intermediates in the aqueous-phase reforming of sorbitol. *ChemSusChem*, 3(6):708–718, 2010. ISSN 1864-564X. doi: 10.1002/cssc.200900254.

[20] Bernard M. Kabyemela, Tadafumi Adschiri, Roberto M. Malaluan, and Kunio Arai. Glucose and fructose decomposition in subcritical and supercritical water: detailed reaction pathway, mechanisms, and kinetics. *Industrial & Engineering Chemistry Research*, 38(8):2888–2895, 1999. ISSN 0888-5885. doi: 10.1021/ie9806390.

[21] Aaron K. Goodwin and Gregory L. Rorrer. Conversion of glucose to hydrogen-rich gas by supercritical water in a microchannel reactor. *Industrial & Engineering Chemistry Research*, 47(12):4106–4114, 2008. ISSN 0888-5885. doi: 10.1021/ie701725p.

[22] Taku Michael Aida, Kiyohiko Tajima, Masaru Watanabe, Yuki Saito, Kiyoshi Kuroda, Toshiyuki Nonaka, Hideo Hattori, Richard Lee Smith Jr, and Kunio Arai. Reactions of d-fructose in water at temperatures up to 400 c and pressures up to 100 mpa. *The Journal of Supercritical Fluids*, 42(1):110–119, 2007. ISSN 0896-8446. doi: 10.1016/j.supflu.2006.12.017.

[23] A. Kruse and A. Gawlik. Biomass conversion in water at 330410 c and 3050 mpa. identification of key compounds for indicating different chemical reaction pathways. *Industrial & Engineering Chemistry Research*, 42(2):267–279, 2003. ISSN 0888-5885. doi: 10.1021/ie0202773.

[24] Bernard M. Kabyemela, Tadafumi Adschiri, Roberto M. Malaluan, and Kunio Arai. Kinetics of glucose epimerization and decomposition in subcritical and supercritical water. *Industrial & Engineering Chemistry Research*, 36(5):1552–1558, 1997. ISSN 0888-5885. doi: 10.1021/ie960250h.

[25] Ning Li, Geoffrey A Tompsett, Taiying Zhang, Jian Shi, Charles E Wyman, and George W Huber. Renewable gasoline from aqueous phase hydrodeoxygenation of aqueous sugar solutions prepared by hydrolysis of maple wood. *Green Chemistry*, 13(1):91–101, 2011. doi: 10.1039/C0GC00501K.

[26] Prabir Basu. Chapter 4 - tar production and destruction. In Prabir Basu, editor, *Biomass Gasification and Pyrolysis*, pages 97 – 116. Academic Press, Boston, 2010. ISBN 978-0-12-374988-8. doi: http://dx.doi.org/10.1016/B978-0-12-374988-8.00004-0.

[27] Athika Chuntanapum and Yukihiko Matsumura. Char formation mechanism in supercritical water gasification process: A study of model compounds. *Industrial & Engineering Chemistry Research*, 49(9):4055–4062, 2010. ISSN 0888-5885. doi: 10.1021/ie901346h.

[28] Athika Chuntanapum and Yukihiko Matsumura. Formation of tarry material from 5-hmf in subcritical and supercritical water. *Industrial & Engineering Chemistry Research*, 48(22):9837–9846, 2009. ISSN 0888-5885. doi: 10.1021/ie900423g.

[29] X. H. Hao, L. J. Guo, X. Mao, X. M. Zhang, and X. J. Chen. Hydrogen production from glucose used as a model compound of biomass gasified in supercritical water. *International Journal of Hydrogen Energy*, 28(1):55–64, 2003. ISSN 0360-3199. doi: 10.1016/S0360-3199(02)00056-3.

[30] Anand G. Chakinala, Jithendra K. Chinthaginjala, Kulathuiyer Seshan, Wim P. M. van Swaaij, Sascha R. A. Kersten, and Derk W. F. Brilman. Catalyst screening for the hydrothermal gasification of aqueous phase of bio-oil. *Catalysis Today*, 195(1):83–92, 2012. ISSN 0920-5861. doi: http://dx.doi.org/10.1016/j.cattod.2012.07.042.

[31] National Institute of Standards and Technology. URL `http://webbook.nist.gov/chemistry/`.

[32] Dortmund Data Bank Software & Separation Technology. URL `http://ddbonline.ddbst.de/AntoineCalculation/AntoineCalculationCGI.exe?component=Water`.

[33] M. van Lotringen. Hydrotreatment of aqueous glucose solutions, master thesis, university of twente. 2011.

Appendix A

HPLC calibration curves for sorbitol and glucose

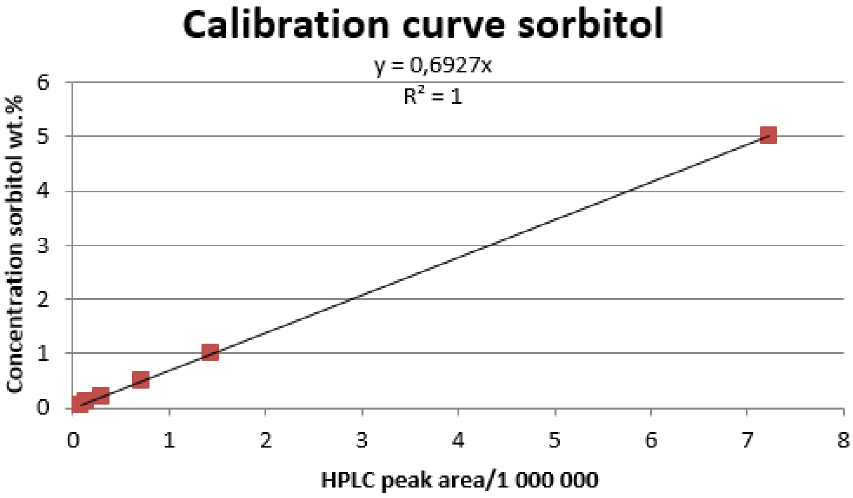

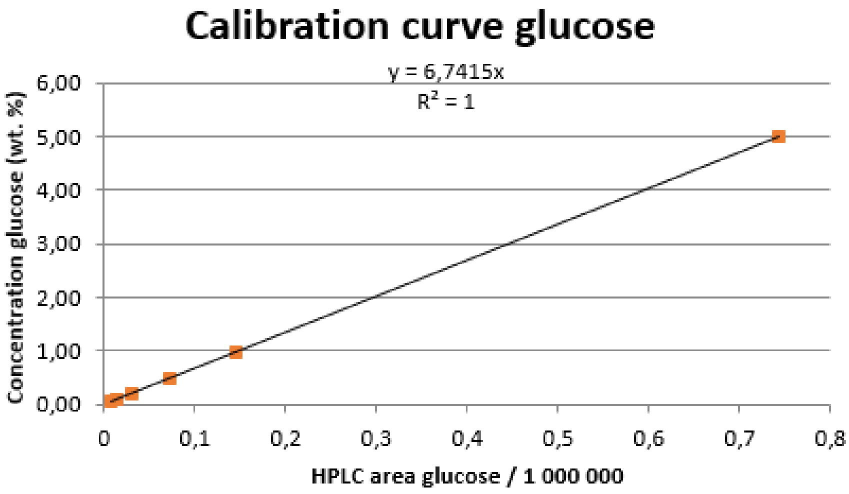

Appendix B

GC-MS results

Ethyl acetate extract

```
  Data Path : C:\msdchem\1\data\varsha\20150622 different solvents\
  Data File : exp8-ethyl acetate.D
  Acq On    : 22 Jun 2015  10:31
  Operator  : stijn
  Sample    : exp8-ethyl acetate
  Misc      :
  ALS Vial  : 8   Sample Multiplier: 1

  Search Libraries:   C:\Database\Wood.L                Minimum Quality:
40
                      C:\Database\NIST08.L              Minimum Quality:
0

  Unknown Spectrum:   Apex
  Integration Events: ChemStation Integrator - autoint1.e

Pk#     RT  Area%          Library/ID                  Ref#     CAS#   Qual
___________________________________________________________________________
__
  1   7.799  3.94 C:\Database\Wood.L
                 ORT-Nr.016; Acetic acid; RT 7,956      16 000064-19-7 72
                 min
                 ORT-Nr.146.1; 1,6-Anhydro-galactop    190 000644-76-8  4
                 yranose; RT 58,820 min
                 ORT-Nr.159; Levoglucosan; RT 59,25    159 000498-07-7  2
                 6 min

  2   7.899  4.57 C:\Database\NIST08.L
                 n-Propyl acetate                     4217 000109-60-4 32
                 Propanal, 2,3-dihydroxy-, (S)-       2258 000497-09-6  9
                 5-Methyloxazolidine                  1869 058328-22-6  9

  3   8.105  1.79 C:\Database\NIST08.L
                 3-Pentanone                          1704 000096-22-0 43
                 3-Pentanone                          1698 000096-22-0 38
                 6-Hepten-3-one, 5-hydroxy-4,6-dime  28545 062338-59-4 28
                 thyl-

  4  11.776  2.32 C:\Database\Wood.L
                 ORT-Nr.021; Propanoic acid; RT 12,     21 000079-09-4 45
                 258 min
                 ORT-Nr.019; Acetoin; RT 10,521 min     19 000513-86-0  1
                 ORT-Nr.002; Formaldehyde; RT 3,195      2 000050-00-0  1
                  min

  5  13.149  2.19 C:\Database\Wood.L
                 ORT-Nr.024; Cyclopentanone; RT 13,     24 000120-92-3 78
                 300 min
                 ORT-Nr.067; 2(5H)-Furanone; RT 25,     67 000497-23-4  3
                 560 min
```

```
 6  16.342 13.77 C:\Database\Wood.L
                ORT-Nr.040; 2-Cyclopenten-1-one; R     40 000930-30-3 94
                T 16,389 min
                ORT-Nr.007; Furan, 2-methyl-; RT 5      7 000534-22-5 32
                ,220 min
                ORT-Nr.022; Furan, 3-methyl-; RT 1     22 000930-27-8 12
                2,395 min

 7  19.234  9.33 C:\Database\Wood.L
                ORT-Nr.051; 2-Cyclopenten-1-one, 2     51 001120-73-6 91
                -methyl-; RT 19,440 min
                ORT-Nr.065; 2-Cyclopenten-1-one, 3     65 002758-18-1 72
                -methyl-; RT 24,930 min
                ORT-Nr.037; 2-Furaldehyde; RT 16,7     37 000098-01-1  9
                00 min

 8  20.069  6.92 C:\Database\Wood.L
                ORT-Nr.054; Ethanone, 1-(2-furanyl     54 001192-62-7 78
                )-; RT 20,286 min
                ORT-Nr.050; 4,4-Dimethyl-2-cyclope     50 022748-16-9  5
                nten-1-one; RT 19,143 min
                ORT-Nr.034; 3-Furaldehyde; RT 15,0     34 000498-60-2  2
                03 min

 9  24.196  2.36 C:\Database\Wood.L
                ORT-Nr.065; 2-Cyclopenten-1-one, 3     65 002758-18-1 87
                -methyl-; RT 24,930 min
                ORT-Nr.051; 2-Cyclopenten-1-one, 2     51 001120-73-6 72
                -methyl-; RT 19,440 min
                ORT-Nr.077; 4H-Pyran-4-one; RT 28,     77 000108-97-4  4
                224 min

10  26.860  1.25 C:\Database\Wood.L
                ORT-Nr.074; 2-Cyclopenten-1-one, 2     74 001121-05-7 86
                ,3-dimethyl-; RT 27,675 min
                ORT-Nr.125; Catechol; 1,2-Benzened    125 000120-80-9  9
                iol; RT 44,874 min
                ORT-Nr.137; Hydroquinone; RT 48,15    137 000123-31-9  7
                0 min

11  26.965 27.40 C:\Database\NIST08.L
                Cyclopropane, pentyl-                6624 002511-91-3 94
                1-Octanol                           13482 000111-87-5 91
                1-Octanol                           13475 000111-87-5 87

12  28.901  1.99 C:\Database\Wood.L
                ORT-Nr.080; Phenol; RT 29,835 min      80 000108-95-2 86
                ORT-Nr.082.1; 2-Cyclopenten-1-one,    199 005682-69-9  1
                 3-ethyl-; RT 30,789 min
                ORT-Nr.082.1; 2-Cyclopenten-1-one,    198 005682-69-9  1
                 3-ethyl-; RT 30,789 min

13  44.169 22.15 C:\Database\NIST08.L
                Isosorbide                          21490 000652-67-5 95
                Isosorbide                          21491 000652-67-5 95
                Dianhydromannitol                   21495 1000127-66-7 80
```

Hexane extract

```
  Data Path : C:\msdchem\1\data\varsha\20150610 test hexane\
  Data File : exp 8 hexane extracted.D
  Acq On    : 10 Jun 2015  18:09
  Operator  : stijn
  Sample    : exp 8 hexane extracted
  Misc      :
  ALS Vial  : 7   Sample Multiplier: 1

  Search Libraries:   C:\Database\Wood.L               Minimum Quality:
40
                      C:\Database\NIST08.L             Minimum Quality:
0

  Unknown Spectrum:   Apex
  Integration Events: ChemStation Integrator - autoint1.e

Pk#     RT  Area%          Library/ID                  Ref#     CAS#   Qual
___________________________________________________________________________
__
  1   8.523  0.78 C:\Database\NIST08.L
                 Acetic acid                            263 000064-19-7 91
                 Acetic acid                            262 000064-19-7 90
                 Ammonium acetate                       976 000631-61-8 83

  2   9.741  0.19 C:\Database\Wood.L
                 ORT-Nr.017; Acetol;  RT9,090 min        17 000116-09-6 80
                 ORT-Nr.026; 3-Hydroxypropanal; RT       26 000000-00-0  9
                 13,626 min
                 ORT-Nr.036; x-Hydroxy-oxo-butanal;      36 000000-00-0  9
                  RT 16,005 min

  3  16.393  1.52 C:\Database\Wood.L
                 ORT-Nr.040; 2-Cyclopenten-1-one; R      40 000930-30-3 94
                 T 16,389 min
                 ORT-Nr.022; Furan, 3-methyl-; RT 1      22 000930-27-8 37
                 2,395 min
                 ORT-Nr.007; Furan, 2-methyl-; RT 5       7 000534-22-5 23
                 ,220 min

  4  19.258  0.45 C:\Database\Wood.L
                 ORT-Nr.051; 2-Cyclopenten-1-one, 2      51 001120-73-6 91
                 -methyl-; RT 19,440 min
                 ORT-Nr.065; 2-Cyclopenten-1-one, 3      65 002758-18-1 58
                 -methyl-; RT 24,930 min
                 ORT-Nr.037; 2-Furaldehyde; RT 16,7      37 000098-01-1  5
                 00 min

  5  20.081  0.36 C:\Database\Wood.L
                 ORT-Nr.054; Ethanone, 1-(2-furanyl      54 001192-62-7 91
                 )-; RT 20,286 min
                 ORT-Nr.050; 4,4-Dimethyl-2-cyclope      50 022748-16-9 78
                 nten-1-one; RT 19,143 min
                 ORT-Nr.034; 3-Furaldehyde; RT 15,0      34 000498-60-2  1
                 03 min

  6  26.983  0.43 C:\Database\Wood.L
                 ORT-Nr.073; 2-Cyclopenten-1-one, 2      73 000080-71-7 95
                 -hydroxy-3-methyl-; RT 28,008 min
                 ORT-Nr.082; 3-Furancarboxylic acid      82 000488-93-7  9
                 ; RT 30,492 min
```

```
                ORT-Nr.096; 2-Furancarboxylic acid     96 000088-14-2  5
                ; RT 35,802 min

 7  34.269  0.68 C:\Database\NIST08.L
                Pentanoic acid, 4-oxo-               7955 000123-76-2 91
                Pentanoic acid, 4-oxo-               7954 000123-76-2 91
                Pentanoic acid, 4-oxo-               7953 000123-76-2 91

 8  37.990  1.02 C:\Database\NIST08.L
                Dianhydromannitol                   21495 1000127-66-7 64
                N-Carbobenzoxy-l-alanyl-glycyl-gly 163188 1000133-12-7 40
                cine
                N-dl-Leucylglycine                  50616 000615-82-7 38

 9  44.698 77.44 C:\Database\NIST08.L
                Isosorbide                          21490 000652-67-5 96
                Isosorbide                          21491 000652-67-5 95
                Dianhydromannitol                   21495 1000127-66-7 86

10  46.389  0.69 C:\Database\NIST08.L
                Ethanethioic acid, S-(tetrahydro-2  30481 035890-63-2 35
                H-pyran-3-yl) ester
                1,3;2,5-Dimethylene-l-rhamnitol     52006 1000128-41-1 27
                2-Pyrrolidinecarboxamide, 5-oxo-,   11927 016395-57-6 25
                (S)-

11  48.986  3.60 C:\Database\NIST08.L
                Isosorbide                          21490 000652-67-5 97
                Isosorbide                          21491 000652-67-5 95
                Dianhydromannitol                   21495 1000127-66-7 72

12  49.164  0.41 C:\Database\Wood.L
                ORT-Nr.148; 5-Methyl resorcinol (H    148 000504-15-4 58
                ydrat); RT 53,433 min
                ORT-Nr.130; 3-Methyl catechol; RT     130 000488-17-5 58
                46,800 min
                ORT-Nr.059; Phenol, 3-methoxy-; RT     59 000150-19-6  1
                 22,725 min

13  50.282  0.34 C:\Database\NIST08.L
                Ketone, methyl 2,2,3-trimethylcycl  26351 017983-22-1 38
                opentyl
                4,5-Octanediol, 2,7-dimethyl-       39996 1000153-20-8 35
                Furan, 2,3-dihydro-3-methyl-         1438 001708-27-6 22

14  63.781 12.09 C:\Database\NIST08.L
                Ribo-ribo disaccharide             122080 133008-06-7 47
                1,1-Di(methylthio)cyclobutane       22667 1000250-41-7 42
                Thiazole, 4,5-dihydro-2-(methylthi  14436 019975-56-5 25
                o)-
```

Octanol extract

```
  Data Path : C:\msdchem\1\data\varsha\20150622 different solvents\
  Data File : exp8- octanol.D
  Acq On    : 22 Jun 2015  12:21
  Operator  : stijn
  Sample    : exp8- octanol
  Misc      :
  ALS Vial  : 9   Sample Multiplier: 1

  Search Libraries:   C:\Database\Wood.L                Minimum Quality:
40
                      C:\Database\NIST08.L              Minimum Quality:
0

  Unknown Spectrum:   Apex
  Integration Events: ChemStation Integrator - autoint1.e

Pk#     RT  Area%          Library/ID                  Ref#     CAS#   Qual
___________________________________________________________________________
__
  1   3.343  0.05 C:\Database\NIST08.L
                   Methane                                5 000074-82-8  2
                   Methane                                4 000074-82-8  2
                   Methane                                3 000074-82-8  2

  2   3.582  0.83 C:\Database\NIST08.L
                   Ammonia                                6 007664-41-7  2
                   Water                                  7 007732-18-5  1

  3   3.971  0.02 C:\Database\Wood.L
                   ORT-Nr.004; Furan; RT 4,194 min        4 000110-00-9 86
                   ORT-Nr.076; 2H-Pyran-2-one; RT 28,    76 000504-31-4 74
                   348 min
                   ORT-Nr.055.1; 2-Cyclohexen-1-one;    174 000930-68-7  1
                   RT 21,897 min

  4   4.255  0.05 C:\Database\NIST08.L
                   Acetone                              215 000067-64-1 86
                   Acetone                              214 000067-64-1 83
                   Acetone                              212 000067-64-1 78

  5   5.567  0.10 C:\Database\Wood.L
                   ORT-Nr.011; 2-Butanone; RT 5,616 m    11 000078-93-3 91
                   in
                   ORT-Nr.064; Butanal, 2-ethyl-; RT     64 000097-96-1 36
                   24,005 min
                   ORT-Nr.005; Pyruvaldehyde; RT 4,33     5 000078-98-8  2
                   5 min

  6  16.780  0.08 C:\Database\NIST08.L
                   1-Hexanol                           4379 000111-27-3 90
                   1-Hexanol                           4378 000111-27-3 90
                   1-Hexanol                           4370 000111-27-3 83

  7  29.072 98.29 C:\Database\NIST08.L
                   1-Octanol                          13482 000111-87-5 91
                   1-Octanol                          13483 000111-87-5 91
                   1-Octanol                          13475 000111-87-5 90

  8  29.623  0.09 C:\Database\Wood.L
```

```
                ORT-Nr.080; Phenol; RT 29,835 min      80 000108-95-2 43

 9  31.225  0.10 C:\Database\NIST08.L
                1-Methoxydecane                     38903 007289-52-3 86
                Methyl decyl ether                  38908 1000130-73-4 86
                Cyclopentane, pentyl-               17761 003741-00-2 83

10  32.120  0.08 C:\Database\NIST08.L
                1-Nonanol                           20794 000143-08-8 80
                1-Nonanol                           20804 000143-08-8 80
                Cyclopentane, 1,2-dimethyl-, cis-    3380 001192-18-3 62

11  32.960  0.08 C:\Database\NIST08.L
                Undecane                            27916 001120-21-4 78
                Tridecane                           47621 000629-50-5 74
                Tridecane                           47618 000629-50-5 74

12  36.965  0.10 C:\Database\NIST08.L
                Decanoic acid, methyl ester         48825 000110-42-9 97
                Decanoic acid, methyl ester         48833 000110-42-9 95
                Decanoic acid, methyl ester         48835 000110-42-9 91

13  44.179  0.14 C:\Database\NIST08.L
                Isosorbide                          21490 000652-67-5 97
                Isosorbide                          21491 000652-67-5 95
                Dianhydromannitol                   21495 1000127-66-7 86
```